universität wien

MASTERARBEIT / MASTER'S THESIS

Titel der Masterarbeit / Title of the Master's Thesis

„Lung cancer: Chemosensitivity and PD-L1 expression of primary Non-Small Cell Lung (NSCLC) Cancer cell lines“

verfasst von / submitted by

Adelina Sophia Plangger, BSc

angestrebter akademischer Grad / in partial fulfilment of the requirements for the degree of

Master of Science (MSc)

Wien, 2019 / Vienna 2019

Studienkennzahl lt. Studienblatt / degree programme code as it appears on the student record sheet:	UA 066 834
Studienrichtung lt. Studienblatt / degree programme as it appears on the student record sheet:	Masterstudium Molekulare Biologie
Betreut von / Supervisor:	Ao. Univ.-Prof. Dr. Robert Zeillinger

Acknowledgement

At first, I would like to thank my thesis advisor Ao. Univ.-Prof. Dr. Robert Zeillinger for his supervision of this master thesis and for introducing me to Ao. Univ.-Prof. Dr. Gerhard Hamilton. Thank you both for your excellent guidance and support through each stage of the process.

Next, I would like to thank every patient who contributed pleura effusion to the lung cancer research of Dr. Hamilton and to my work. Thank you, Dr. Maximilian Hochmair for your selfless commitment for helping and treating patients with lung cancer and providing me with numerous samples for my master thesis.

I also want to thank my colleagues here at the Medical University of Vienna for supporting and teaching me not only science related skills but also for answering every question I had. I also owe a big thank you to my friends for their great support. Especially, thank you Ella for your time, your passion, your commitment and for pushing me over my limits during this process.

At last, I want to thank my parents Beate and Andreas and my brothers Attila, Richard and Alwin for their support and help during this time. I could not have done this without knowing that I can count on you.

Abstract

Approximately 85% of lung cancer cases represent Non-small Cell Lung Cancer (NSCLC). The classical therapy for the treatment of NSCLC consists of a platinum-based drug (cisplatin or carboplatin) in combination with either docetaxel, etoposide or pemetrexed, but these regimens of combination chemotherapy result in a low 5-year survival rate of about 20%. Patients who exhibit mutations in driver kinases such as EGFR, ALK or ROS1 are amenable to targeted therapy with specific tyrosine kinase inhibitors (TKIs) yielding improved survival for more than 5 years. Still, patients progressing under TKI therapy have to be treated with cytotoxic chemotherapy. Chemoresistance via different mechanisms is frequently observed in patients treated with platinum-based drugs. In the present study, the sensitivity of PD-L1-negative primary pleural NSCLC and permanent lung cancer cell lines was investigated using proliferation assays, immunofluorescence tests, polymerase chain reaction (PCR) and Western blot arrays. Results of cisplatin cytotoxicity tests demonstrate that most of the pleural NSCLC lines exhibit IC_{50} values of approximately 3 µg/ml which are near the clinical peak plasma concentration (PPC) of the drug and indicate chemoresistance. The NSCLC to Small Cell Lung Cancer (SCLC) transformed pleural cell lines BH659 and BH686 proved to be highly chemosensitive. In order to enhance the cytotoxic effects of cisplatin, combinations with the Chk-1/2 inhibitor AZD-7762, HSP90 inhibitor STA9090, Nrf-2 inhibitor ML385, multitarget inhibitor niclosamide and signal transduction inhibitor pristimerin were performed. AZD-7762 targeting DNA damage response and multitarget niclosamide gave the highest rate of synergistic cytotoxicity with cisplatin but several cancer lines and the other modulators yielded negative results. To expand the cytotoxicity tests to a more representative *in vivo*-like tumor model, 3D spheroids generated on agarose-coated culture flasks were tested. Most cell lines exhibited increased resistance to cisplatin in form of 3D cultures and, with exception of some niclosamide combinations, the modulators were less efficient against such cellular aggregates. Distinct phosphorylation sites of Chk-2, ERK1/2, AKT1/2/3, c-Jun, STAT3 and HSP60 protein expression were assessed with Western blot arrays. Chk-2, c-Jun, STAT3 and HSP60 showed the most frequent increases in phosphorylation in response to pretreatment of the cells with cisplatin. The cisplatin-enhanced phosphorylation or protein expression was higher in cell lines exhibiting basal levels of phosphorylation in the beginning. The transformed cell lines BH659 and BH686 revealed low and uniform increases of the phosphorylation status of the same proteins and

their actual transformation to a SCLC phenotype was confirmed by the proof of the expression of typical markers such as chromogranin A (CHGA), synaptophysin (SYP) and ENO-2 by qPCR.

In conclusion, the primary pleural NSCLC lines show high resistance to cisplatin, independently of the mode of clinical pretreatment and this refractoriness could not be efficiently reversed by a range of modulators in 2D and with even less potency in 3D cultures. In a recent attempt to improve the clinical efficacy of chemotherapy for NSCLC patients, the classical chemotherapeutics were combined with immune checkpoint monoclonal antibodies directed to PD-L1 and PD-1 resulting in improved progression-free and overall survival independently of checkpoint marker expression. Therefore, in the absence of suitable markers for the prediction of the efficacy of an immunochemotherapy treatment, assessment of the cisplatin sensitivity or phosphorylation status of Chk-1/2 as shown in the present work may be useful to select suitable patients for further studies.

Zusammenfassung

Der nicht-kleinzellige Lungenkrebs (NSCLC) macht zirka 85% der Lungenkrebsarten aus. Die klassische Therapiemöglichkeit zur Behandlung von Lungenkrebs besteht aus platinbasierten Medikamenten (Cisplatin oder Carboplatin) in Kombination mit Docetaxel, Etoposid oder Pemetrexed, aber bisher beträgt die 5-Jahres-Überlebensrate trotz dieser Kombination nur rund 20%. Patienten, die eine Mutation in einer „Treiber Kinase“ wie EGFR, ALK oder ROS1 haben, sind empfänglich für gezielte Therapien mit spezifischen Tyrosin Kinase Inhibitoren (TKIs) was zu einem verbesserten Überleben mit mehr als 5 Jahren führen kann. Dennoch müssen Patienten, die unter TKI Behandlung einen Progress erleiden, mit einer zytotoxischen Chemotherapie behandelt werden. Chemoresistenz wird oft bei Patienten beobachtet, die mit platinbasierten Medikamenten behandelt wurden. In dieser Arbeit wurde die Sensitivität von PD-L1 negativen primären NSCLC und permanenten Lungenkrebs Linien mittels Proliferationsassays, Immunofluoreszenztests, Polymerasekettenreaktion und Westernblot Arrays untersucht. Die Ergebnisse der Cisplatin Zytotoxizitätstests zeigen, dass die meisten pleuralen NSCLC Linien IC_{50} Werte aufweisen, die nahe bei 3 µg/ml liegen. Dieser Wert entspricht in etwa der klinischen Spitzenplasmakonzentration und indiziert deshalb Chemoresistenz der Zellen. Die NSCLC zu SCLC transformierten Pleurazelllinien BH659 und BH686 erwiesen sich als hoch chemosensitiv. Um die zytotoxische Wirkung von Cisplatin zu verstärken, wurden Kombinationen mit dem Chk-1/2-Inhibitor AZD-7762, dem HSP90-Inhibitor STA9090, dem Nrf-2-Inhibitor ML385, dem Multitargetinhibitor Niclosamid und dem Signaltransduktionshemmer Pristimerin durchgeführt. AZD-7762, das eine Initiation der Reparatur der DNA Schäden inhibiert, und Multitarget Niclosamid ergaben die höchste Rate synergistischer Zytotoxizität in Kombination mit Cisplatin, während Versuche mit mehreren Krebslinien und anderen Modulatoren negative Ergebnisse lieferten. Um die Zytotoxizitätstests auf ein repräsentativeres *in vivo*-ähnliches Tumormodell auszudehnen, wurden 3D-Aggregate getestet, die in mit Agarose beschichteten Kulturflaschen kultiviert wurden. Die meisten Linien zeigten eine erhöhte Resistenz gegen Cisplatin als 3D-Aggregate und mit Ausnahme von Niclosamid Kombinationen waren die Modulatoren gegenüber solchen Zellaggregaten weniger wirksam. Mittels Westernblot Arrays wurden die spezifischen Phosphorylierungsstellen von Chk-2, ERK1/2, AKT1/2/3, c-Jun, STAT3 und die Proteinexpression von HSP60 untersucht. Chk-2, c-Jun, STAT3 und HSP60 zeigten die

häufigsten Anstiege der Phosphorylierung oder Proteinexpression als Reaktion auf die Vorbehandlung der Zellen mit Cisplatin. Die Cisplatin-induzierte Phosphorylierung wurde in Zelllinien verstärkt, die zu Beginn basale Phosphorylierungsgrade aufwiesen. Die transformierten Zelllinien BH659 und BH686 zeigten eine geringe und gleichmäßige Erhöhung des Phosphorylierungsstatus derselben Proteine. Ihre tatsächliche Transformation in einen SCLC-Phänotyp wurde durch den Nachweis der Expression typischer Marker wie CHGA, SYP und ENO-2 mittels qPCR bestätigt.

Zusammenfassend lässt sich sagen, dass die primären pleuralen NSCLC Linien unabhängig von der Art der klinischen Vorbehandlung eine hohe Resistenz gegen Cisplatin aufweisen und dass diese Resistenz durch eine Reihe von Modulatoren in 2D und mit noch geringerer Wirksamkeit in 3D-Kulturen nicht effizient rückgängig gemacht werden kann. In einem kürzlich unternommenen Versuch, die klinische Wirksamkeit der Chemotherapie bei NSCLC-Patienten zu verbessern, wurden die klassischen Chemotherapeutika mit monoklonalen Antikörpern gegen PD-L1 und PD-1 kombiniert, was unabhängig von der Checkpoint-Marker-Expression zu einem verbesserten progressionsfreien Überleben führte. In Abwesenheit geeigneter Marker für die Vorhersage der Wirksamkeit einer Immunchemotherapie kann daher die Beurteilung der Cisplatinsensitivität oder des Phosphorylierungsstatus von Chk-1/2, wie in der vorliegenden Arbeit gezeigt, nützlich sein, um geeignete Patienten für weiterführende Studien auszuwählen.

Table of contents

1 Introduction

1.1 Lung cancer

According to the World Health Organization cancer is defined as *"[…] a generic term for a large group of diseases that can affect any part of the body. Other terms used are malignant tumors and neoplasms. One defining feature of cancer is the rapid creation of abnormal cells that grow beyond their usual boundaries, and which can then invade adjoining parts of the body and spread to other organs, the latter process is referred to as metastasizing."* (WHO, 2018)

Today, cancer has become a leading cause of death worldwide. Aging is one of the most important factors because the risk of tumorigenesis accumulates with increasing age. In elder people cells tend to repair damages less effective compared to younger individuals. However, a high body mass index, low fruit and vegetable intake, tobacco and alcohol use as well as lack of physical activity are also important risk factors. Especially, tobacco usage is the most important factor for developing cancer and is accountable for about 22% of cancer related deaths. Cancer burden can be reduced by avoiding or reducing the risk factors such as by quitting tobacco usage, losing weight and starting a healthy diet. Early detection of cancer and screening programs are also related with better patient survival, less morbidity and more effective treatment.

It is estimated that in 2018 about 9.6 million people died of cancer, this equals 1 in 6 deaths. Lung cancer was the most reported cancer with around 2.09 million cases followed by breast and colorectal cancer. In 2018 approximately 1.76 million people died of lung cancer worldwide (WHO, 2018).

Figure 1 illustrates the numbers of newly reported lung cancer cases over the last decade in Austria.

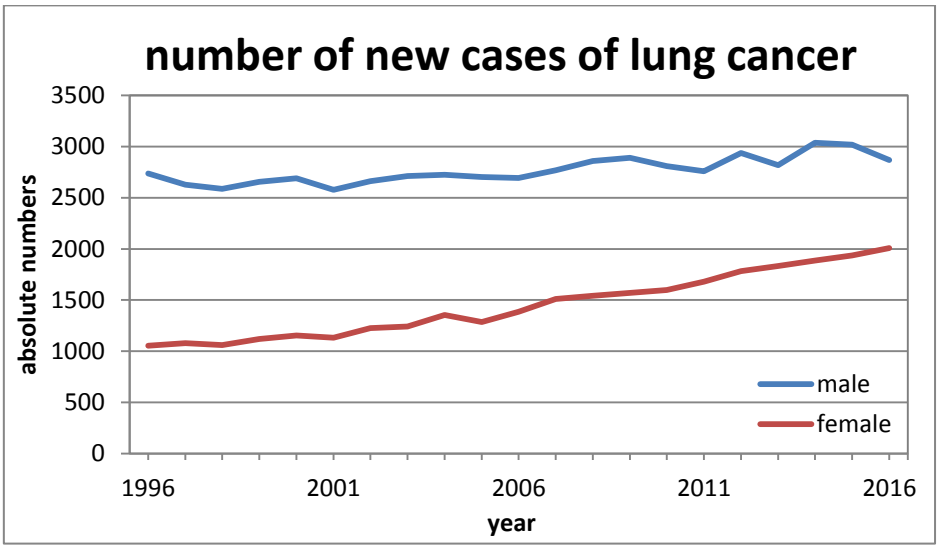

Figure 1 absolute numbers of new incidences of lung cancer from 1996 to 2016 in Austria.

Lung cancer is the second most common cancer type in men and women in Austria and is the reason for most cancer deaths in men and the second most common cancer deaths in women. In 2015 4860 people were diagnosed with lung cancer, while 3889 cancer patients died in Austria. The number of new cases in men stayed almost constant. Unfortunately, the number of new incidences in women doubled in 2016 compared to 1996. The same trend could also be observed for the cases of lung cancer mortality. The number in men remained around 2400 from 1996 to 2016. However, the number of women who died of lung cancer drastically increased over the last ten years (Figure 2). In half of all new reported cases the cancer was diagnosed when already disseminated into other tissues. In almost 30% of the cases no definitive tumor state could be determined (20% unknown tumor state, 9% death-certificate-only cases) (Statistics Austria, 2018a, 2018b, 2019).

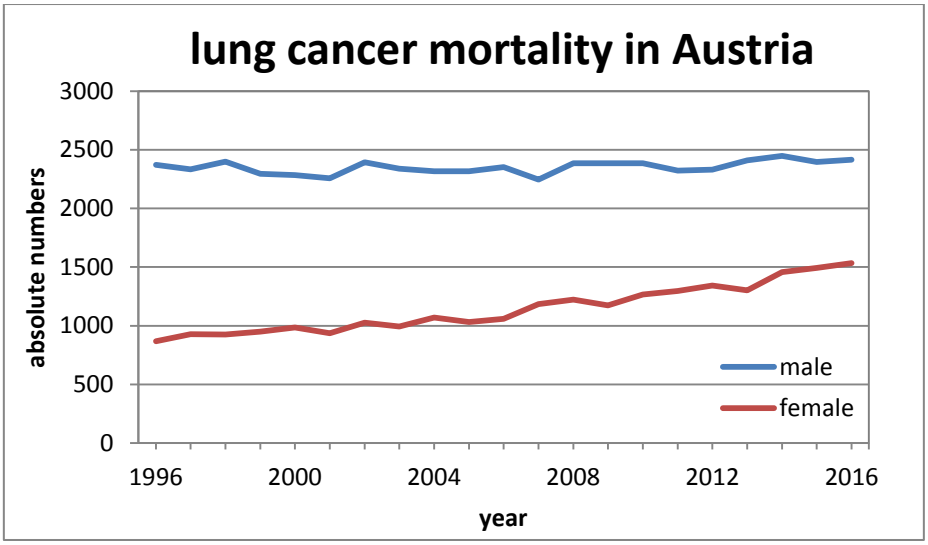

Figure 2 absolute numbers of incidences of lung cancer deaths from 1996 to 2016 in Austria.

Smoking and usage of tobacco products is the most common and the most preventable risk factor for lung cancer. Eventually, every 9th smoker develops lung cancer. It has been suggested that about 20% of lung cancer deaths would be avoidable if patients would quit tobacco smoking (Dela Cruz, Tanoue & Matthay, 2011). According to Statistics Austria, the percentage of smoking in women increased from 17.1% to 23.3% in the time period from 1979 to 1997. In 2014 about 21.1% of the evaluated women were smoking on a daily basis. However, 27.8% women in the age class from 15-30 and 27.9% in the age class of 30-45 were frequent smokers. Therefore, smoking in women increased over the last 35 years whereas in the same period, smoking in men decreased. In 1979 41.1% of the evaluated men were smoking, in 1986 40% and in 1997 only 35.9%. The share in smoking men dropped to 26.5%. However, in 2014 32.2% men in the age class of 15-30 and 33.2% in the age class of 30-45 were frequent smokers, respectively (Statistics Austria 2007, 2015).

Statistics Austria estimates that in 2030 11700 men and 11900 women will be diagnosed with lung cancer. In comparison, in 2014 7200 men and 5200 women were alive with the same diagnosis. Therefore, the numbers of women with lung cancer will increase by 129% and by 64% in men. This trend of a significant increase of lung cancer incidences and mortality in women is a follow-up movement. In the 1960s and 70s women slowly began to conquer male domains and consequently started to smoke. The generation of women born in the 50s and 60s are now at risk of developing lung cancer. For 2020, it is estimated that 2948 new cases of lung cancer in men and 2277 in women will be diagnosed. 10 years later, in 2030 “only” 2958 new incidences in men and 3208 in women are forecast. Currently, about 24.3% of the population in Austria is smoking. Within the EU only Greeks and Hungarians smoke more than Austrians (Austrian Society of Pneumology, 2019).

Long-term smokers have a 10 to 30-fold risk of developing lung cancer compared to lifelong nonsmokers which have a risk of 1% of developing lung cancer during their lifetime. The smoke of cigarettes consists of mainstream and sidestream smoke components as well as gaseous compounds and respirable dust and particles. The main risk factor for the smoker is the smoke which is produced by inhalation of air through the filter after lighting the cigarette. Sidestream smoke is a result of smoldering in between puffs. The total respirable particles, besides nicotine and water of smoke, are identified as tar. It is estimated that a tar exposure is a possible risk for lung cancer development. However, nicotine is the main reason for tobacco addiction (Dela Cruz, Tanoue & Matthay, 2011).

In the 1950s, the tobacco industry instituted filters in order to lower the tar content as they assumed lower tar content equals reduced risks of smoking. Therefore, people who wanted to smoke “healthier” chose cigarettes with lower tar yields. Due to the filter, the impression of a light smoking experience was generated. However, the introduction of the filter resulted in some unpleasant side effects. The smoke mixed with air could be inhaled deeper into the lungs, people could take bigger puffs and larger particles could be delivered more deeply. Also, people got the impression that they could smoke more cigarettes per day. All these new factors caused an increased exposure to the portion of the peripheral lungs (Song et al., 2017). Cigarette smoke contains more than 4000 chemical compounds such as polycyclic aromatic hydrocarbons, aromatic amines, N-nitrosamines, benzene, vinyl chloride, arsenic and chromium. Many of these compounds are known to be potential carcinogens (Dela Cruz, Tanoue & Matthay, 2011).

1.2 Types of lung cancer

In general, lung cancer can be divided into Non-small Cell Lung Cancer (NSCLC) and Small Cell Lung Cancer (SCLC). SCLC shows neuroendocrine properties whereas NSCLC arises from epithelial cells. As of right now, NSCLC accounts for 85% of all lung cancer cases. For a long time, NSCLC and SCLC were used as the most frequent diagnostic terms for lung cancer. There was no need for a morphological differentiation as the treatment possibilities were limited (Osmani et al, 2018). Nowadays, NSCLC is classified into three major histological subtypes: adenocarcinoma (AC), squamous-cell carcinoma (SCC) and large-cell carcinoma. AC accounts for approximately 40% of the cases, SCC for around 25% of the cases and large-cell carcinoma comprises 10% of the cases of lung cancer. The remaining 25% are divided among other types or are not otherwise specified (Figure 3). Over the past decades, significantly more patients with lung cancer were diagnosed with AC instead of SCC. The latter type is histologically characterized by the presence of keratinization shown as squamous pearls and intercellular bridges. This type of cancer grows due to dysplasia and can develop into an invasive form over the time of several years (Rooney, Devarakonda & Govindan, 2013). Smoking is associated with all types of lung cancer but especially with SCLC and SCC (Herbst, Heymach & Lippman, 2008). People smoking cigarettes marketed as "light" or "ultralight" have an increased risk of developing AC (Song et al., 2017).

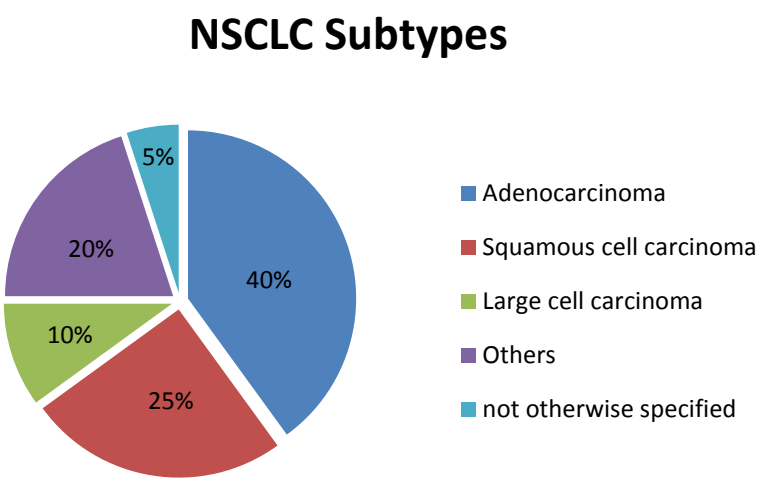

Figure 3 Summary of the different subtypes of NSCLC

1.3 Driver mutations

In 2000 Weinberg and Hanahan published the six hallmarks of cancer: evading apoptosis, self-sufficiency in growth signals, insensitivity to anti-growth signals, sustained angiogenesis, limitless replicative potential and tissue invasion & metastasis. It is established that a tumor cell has to acquire this set of novel capabilities in order to overcome the defense mechanisms of the healthy tissue and effector cells. However, tumorigenesis is not a single event but a multistep process. Every genetic alteration contributes to the progression of a healthy cell into a malignant variant (Hanahan & Weinberg, 2000).

However, many driver mutations are involved in AC occurrence as it can be seen from Figure 4. Unfortunately, nearly 40% of the driver mutations accounting for this type of disease are still unknown.

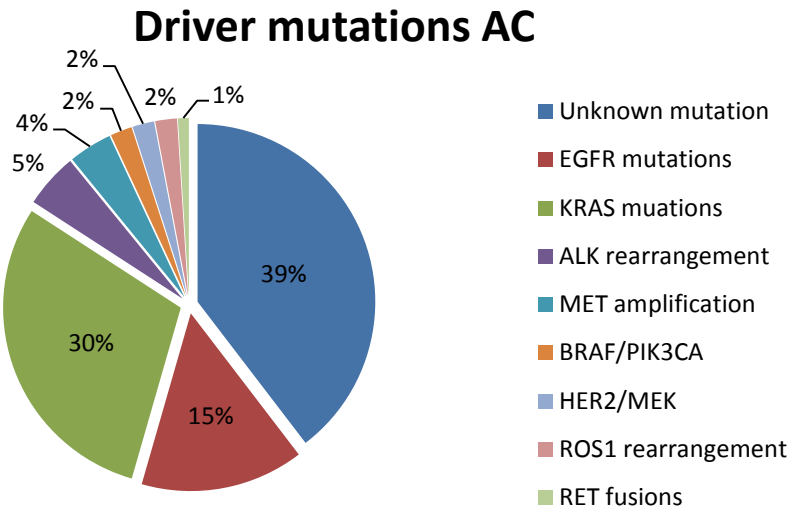

Figure 4 Overview of the driver mutations in AC.

KRAS (Kirsten rat sarcoma 2 viral oncogene homolog), a member of the family of GTPases, is mutated in 30% of the cases, followed by the epidermal growth factor receptor (EGFR) mutations with 15%. EGFR is a member of receptor tyrosine kinases and stimulates downstream pathways which control cell growth, proliferation and cell survival such as RAS/RAF/MEK/ERK, MAPK pathway or PI3K-AKT-mTOR pathway. The activity of EGFR can be altered in three different ways: increased expression on cancer cells, enhanced ligand production by these cells and an activating mutation of this receptor within the altered cells. In 60% of the cases exon 19 is deleted and in 35% leucine is replaced by arginine at position 858. Both mutations lead to an activation of the receptor without the necessity of a binding ligand. The GTPase KRAS can transduce growth signals from different tyrosine kinases. Therefore, a mutation leads to a constitutive activation of growth signals from multiple tyrosine kinases. Mutations of KRAS can be found preferably in

smokers (former or current) and Caucasian people. It is assumed that patients with this type of mutations have a poorer prognosis and an effective therapy remains to be found as it is related with resistance against EGFR tyrosine kinase inhibitors (TKIs) (Chan & Hughes, 2015).

ALK (anaplastic lymphoma kinase) rearrangement is quite common in lung cancer. The transmembrane tyrosine kinase receptor ALK pertains to the insulin receptor family and ensures normal cell proliferation and neurogenesis by interacting and communicating with canonical pathways (MAPK, PI3K-mTOR, JAK/STAT and others) (Liu et al., 2019). Up to now, more than 19 different ALK fusion protein variations were found in NSCLC such as EML4, KIF5B and KLC1. In lung cancer, this gene is often fused to EML4 due to an inversion on chromosome 2p. The fusion protein is controlled by the promotor of EML4 which leads to an overexpression and constitutive activity of the ALK tyrosine kinase. This induces increased cell proliferation, higher metabolism, remodeling of the cytoskeleton and increased migration as well as decreased apoptosis (Hamilton et al. 2019). ALK rearrangement is preferably found in younger patients with AC who were light smokers or non-smokers. It can often be found in tumors not carrying EGFR or KRAS mutations. In about 4% of AC an amplification of mesenchymal-epithelial transition (MET) factor was documented. Due to that amplification, the gene product (HGFR) is overexpressed and deregulates cell proliferation, migration and metastasis. Apparently, MET and EGFR seem to have synergistic properties as the amplification MET can cause acquired EGFR TKI resistance (Chan & Hughes, 2015).

On the other hand, the most common driver mutations in SCC are PIK3CA (phosphatidylinositol 3-kinase) amplification and mutation (34% and 15%, respectively) and the fibroblast growth factor receptor type 1 (FGFR1) pathway which accounts for about 20% (Figure 5) (Chan & Hughes, 2015).

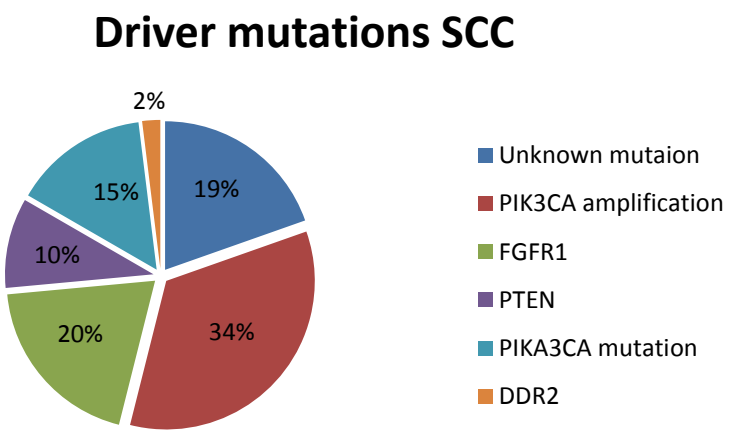

Figure 5 Summary of the driver mutations in SCC.

FGFR1 is important for cell development and can be altered by amplification, translocation or point mutation (Dutt et al., 2011). The loss of PTEN, a tumor suppressor gene, is also a common alteration in SCC. Normally, this phosphatase degrades phosphatidylinositol(3,4,5)triphosphate (PIP_3) in a negative feed-back mechanism and therefore inhibits the PI3K signaling to regulate the proliferation in cells. In case of a loss of function mutation in PTEN, the PI3K signaling amplifies and promotes tumorigenesis (Hanahan & Weinberg, 2011). A mutation in the discoidin domain receptor 2 (DDR2) occurs in 2% of lung cancer cases. This tyrosine kinase receptor and its corresponding ligand collagen are linked to cell migration, survival and proliferation (Chan & Hughes, 2015).

In Figure 6, the affected kinases, receptors and corresponding signaling pathways are shown. A mutation in each one of these mediators can have a quite extensive impact on the signal cascades within pathways.

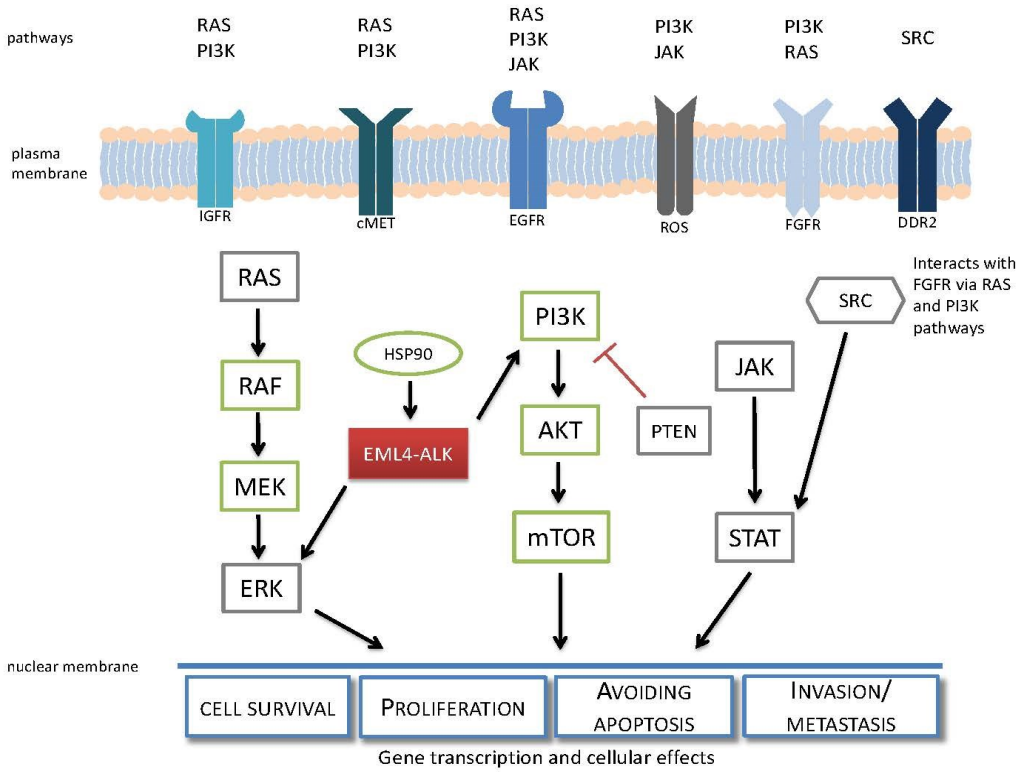

Figure 6 Summary of the pathways and receptors of NSCLC.

The most common affected pathways are involved in cell growth, differentiation, cell survival and proliferation such as RAS/RAF/MERK/ERK, PI3K/AKT/mTOR or JAK/STAT. An alteration of one component of these pathways can have a crucial impact on the cells and subsequently can lead to uncontrolled proliferation, growth and prevention of apoptosis. Furthermore, the mutations can lead to invasion, metastasis as well as promotion of angiogenesis. The so-called invasion-metastasis cascade comprises invasion of tumor cells, intravasation of cancer cells into

lymphatic and blood vessels, transport through the circulation, extravasation at distal tissues and formation of new micrometastases. Eventually, these grow into lesions and macroscopic metastases (Hanahan & Weinberg, 2011). Src kinase (SRC) is a member of the family of non-receptor membrane associated tyrosine kinases. Its normal functions comprise regulation of cell proliferation regulation and maintenance of normal intercellular contacts, regulation of the cytoskeleton, motility and migration. Therefore, in case of a mutation, it can also promote tumor growth as it transfers signals from the extracellular site to the biochemical pathways and have an impact on the reorganization of the cytoskeleton and adhesion properties of the cell. This leads to increased motility and invasion of tumor cells (Guarino, 2010). IGFR, MET, EGFR and ROS are more likely to be altered in AC, mutations in FGFR, SRC, PTEN and DDR2 are more common in SCC (Chan & Hughes, 2015).

Nevertheless, there are significant differences in the frequency of the driver mutations of NSCLC in the US and Europe compared to those in East Asia (Japan, Korea and China). As Figure 7 shows, in the USA and Europe the most common aberration of driver oncogene is KRAS followed by EGFR mutations. The remaining mutations found in AC only accounts only for 2-4% each. About 50% are still unknown or due to mutations not further specified. In East Asia, however, the most common mutations can be found in EGFR (47%). KRAS mutations can only be found in 9% of all cases. In comparison to USA/EU around 32% of the alterations are not further defined (Kohno et al., 2015).

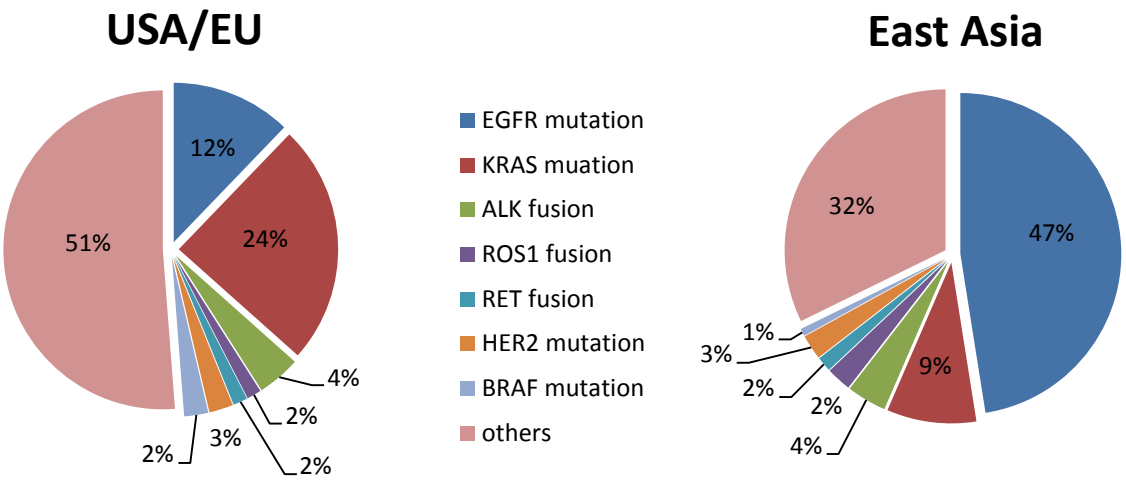

Figure 7 Comparison of the most common driver mutation of AC of USA/ EU and East Asia.

1.4 Survival rates

Roughly 50% of all diagnosed NSCLC cases occur at an advanced stage (stage III or IV) and therefore are not amenable to curative treatment (Tsvetkova & Goss, 2012). The 5-year survival for NSCLC is 60% for localized lung cancer and 33% for regional lung cancer, where the cancer infiltrated tissue outside of the lung or nearby lymph nodes, and 6% for tumors that have already spread across the body and formed metastases (in brain, bones, liver, etc.). The relative 5-year survival rate is 23% for all stages combined (American Cancer Society, 2019). However, the survival rates have improved due to platinum-based doublet chemotherapy. These therapies include combinations of drugs including paclitaxel, docetaxel and pemetrexed with platinum-based drugs (Singh et al., 2016). In comparison, patients diagnosed with SCLC have a poorer prognosis with a rate of 29% for localized, 15% regional and 3% for distant lung cancer. The overall 5-year survival for SCLC is only 6% (American Cancer Society, 2019). It's characteristic for SCLC to disseminate at an early stage. In more than 90% of cases, the tumor spreads and form local advanced or distant metastases. Unfortunately, SCLC is rarely diagnosed at stage I. Only at this point, a surgical treatment can be beneficial for the survival of the patient (Knight et al., 2017). One of the major obstacles to overcome with these therapies is the appearance of drug resistance (Singh et al., 2016).

1.5 Resistance mechanisms

Cancer cells have developed different mechanisms in order to survive drug treatment. The resistance against drugs can be divided in intrinsic or acquired resistance. Intrinsic resistance or innate resistance persists before the treatment of the patient and can lead to a reduced potency of the therapy. This form of resistance can be caused by preexisting mutations leading to a decreased susceptibility to drug regimens in cancer cells, due to heterogeneity of tumor cell populations or activation of pathways that detoxify xenobiotics or external toxins. The extent of intrinsic resistance defines the susceptibility of given tumor cells to a specific drug. However, a genomic analysis of possible drug resistance can help to estimate a specific drug treatment for the needs of a patient (Hamilton & Rath, 2014).

Acquired resistance is defined as the gradual reduction of efficacy of a drug in response to treatment with the drug. This can develop due to activation of a second protooncogene which then becomes the new driver mutation, additional mutations or alterations in the expression of targeted genes or a change in the microenvironment of the tumor. In case of an acquired resistance the drug regimen should be adjusted accordingly (Wang, Zhang & Chen, 2019).

1.5.1 Cellular mechanisms of resistance

The mechanism of drug resistance can be heterogeneous and are more clinically significant while the differentiation of intrinsic or acquired drug resistance is scientifically important. Increased efflux of the drug, alteration of the drug target, enhanced DNA damage repair (DDR), epigenetic alterations, tumor microenvironment (TME), senescence escape, inhibition of cell death and drug inactivation are the most common mechanisms (Figure 8).

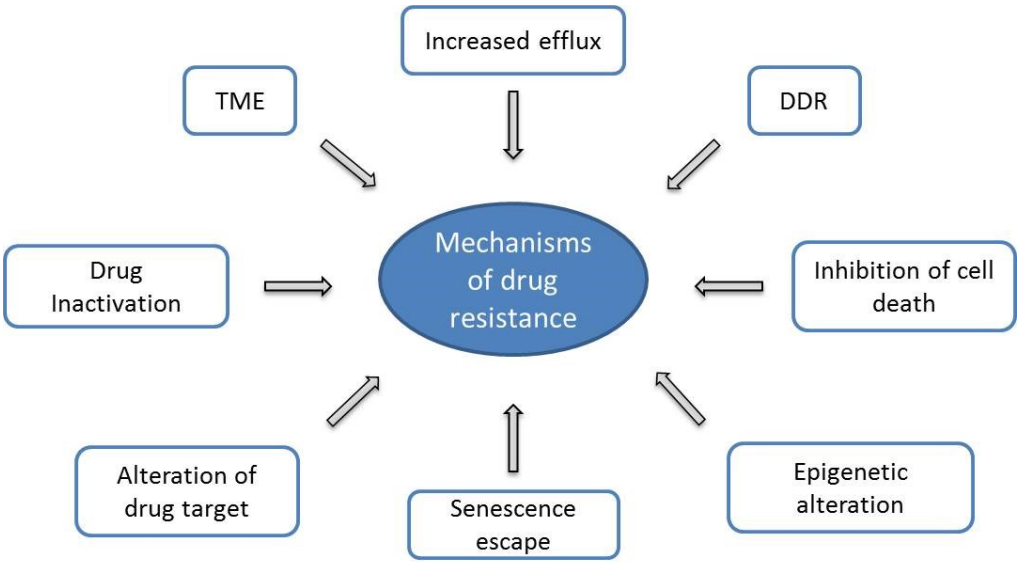

Figure 8 Overview of the different mechanisms of drug resistance (DDR = DNA damage repair, TME = Tumor microenvironment)

Cells tend to increase the efflux of xenobiotics in order to minimize an accumulation of drugs. This mechanism is regarded as one of the reasons for resistance during treatment. Exceedingly high rates of drug effusion can be both intrinsic and acquired as the transmembrane transporters can be altered before and after drug treatment. Primarily, the ABC transporter family is involved in this kind of drug resistance mechanisms as these transporters are responsible for the efflux of drugs. Mutations or overexpression of these transporters can have crucial influence of the susceptibility of the tumor to anticancer drugs as some of these transporters have been identified to be able to transport anti-cancer drugs such as cisplatin derivatives or etoposide. Targeted therapies are designed to effectively and selectively inhibit a specific target protein while being less harmful for normal cells. However, the tumor overcomes this by alteration of the drug target. This includes a secondary mutation in the target protein or a change or modification of expression of the target protein (Wang, Zhang & Chen, 2019). On one hand, the drug target can be altered; on the other hand, the inactivation or absence of activation of drugs can play a crucial role in drug resistance in cancer. Platinum-based drugs, for example, can be inactivated by conjugation with glutathione. Once conjugated, the drug loses its efficacy and can be removed from the cell.

Another mechanism is the lack of activation of a prodrug. A prodrug needs to be converted to its active form which is mostly done by cellular enzymes. The tumor can silence these enzymes resulting in resistance against these drugs as the prodrug cannot be converted (Holohan et al., 2013).

Chemotherapeutic drugs like cisplatin induce DNA damage in cells and therefore lead to apoptosis of the affected cells. The DDR may reduce or even reverse the effect on the cells on account of excision repair or homologous recombination. Apoptosis is crucial for the development and homeostasis of tissues in an organism and can be activated via intrinsic and external pathways. The intrinsic pathway involves BCL-2 family proteins and the extrinsic pathway is stimulated via receptors on the cell surface. Cancer cells tend to overexpress antiapoptotic factors such as BCL-2 family proteins, AKT or highly activated transcription modulators in order to escape the induction of apoptosis (Housman et al., 2014).

In the state of cellular senescence, a cell is arrested in its cell cycle and the activation of tumor suppressive pathways is upregulated. Senescence can be elicited by different external and internal stimuli and also by DNA damage caused by drugs such as cisplatin. An elopement of this induced senescence is regarded as a mechanism for drug resistance (Wang, Zhang & Chen, 2019). Epigenetic altering of the DNA also contributes to resistance of drugs in cancer. The two major types of this alteration are methylation of DNA and alteration of the modification of histones. The latter contributes to the accessibility of histones as acetylation of the terminal lysines opens the chromatin and deacetylation closes them. The methylation of tumor suppressor genes leads to silencing of these genes which also results in resistance. Additionally, oncogenes can be hypermethylated which results in activation of these genes (Mansoori et al., 2017).

A tumor does not consist of homogenous cells but forms a network of different cell types which contribute to tumor growth. The surrounding microenvironment plays a crucial role in the supply and survival of the tumor. Especially, acidosis contributes to drug resistance as the pH gradient is reversed in tumor cells compared to normal cells. This acidic extracellular environment of cancer cells may contribute to resistance to anticancer therapies. Tumors can adapt their TME after treatment and as a result the efficacy of a drug is compromised (Wang, Zhang & Chen, 2019). So-called “immune deserts” impair checkpoint inhibitors as the presence of regulatory T cells (Tregs), myeloid-derived suppressor cells, tumor-associated macrophages, cytokines and chemokines establish an immunosuppressive cancer microenvironment. Subsequently, it leads to an inhibition of immune-mediated anti-tumor effects. (Vasan, Baselga & Hyman, 2019)

1.5.2 Cell transformation as a mechanism of resistance

In very rare cases, a transformation of NSCLC to SCLC can occur. According to literature, this happens in 3-15% of cases after or during the treatment with TKIs. In a few rare cases, those patients were treated with immune checkpoint therapy. This suggests that NSCLC with wild-type EGFR is less prone to switching to SCLC compared to NSCLC with mutated EGFR (Dorantes-Heredia, Ruiz-Morales & Cano-García, 2016). The first switch of NSCLC to SCLC was described in 2006. Originally, this patient was diagnosed with AC and exhibited SCLC in a repeat biopsy still carrying the original mutation of EGFR in exon 19 (Oser et al., 2015). Since then, many patients with the same diagnosis have been reported. These SCLCs were determined by morphology and histology by staining for typical SCLC markers such as SYP, CHGA or ENO-2. It can be assumed that this form of SCLC is not an independent secondary cancer as the original mutation is retained. Nevertheless, the responses to EGFR inhibitors are mixed (Hamilton & Rath, 2019).

1.5.3 Physiological mechanisms of resistance

Normally, a tumor grows in a 3D shape and this cellular arrangement results in a heterogeneous exposure to essential nutrients and oxygen but also physical and chemical stress stimuli. 3D *in vitro* cell cultures recapitulate some features of avascular tumor regions. In 3D structures of larger sizes, the outer cell layers exhibit proliferative cells, whereas the inner layers show hypoxic and, eventually, necrotic cells. Additionally, the 3D cell interactions vary significantly from 2D cultures with regard to cell-cell interactions, cell structure, cell adhesion and signaling as well as overall cell function (Weiswald, Bellet & Dangles-Marie, 2015). In order to determine the difference of 2D and 3D cultures, the chemosensitivity to cisplatin was tested alone and in combination with modulators on several primary cell lines derived from pleura effusions in 2D and compared the effects of these compounds on the same cell lines in 3D models.

1.6 Programmed death-ligand 1

The programmed death 1 (PD-1) receptor is expressed by cells of the immune system such as T-cells, Tregs, B cells, activated monocytes, dendritic cells, and others and can bind its ligand programmed death-ligand 1 (PD-L1). This ligand is a transmembrane protein which is constitutively expressed on antigen presenting cells, non-lymphoid organs and non-hematopoietic tissues (heart, lung, placenta and liver). PD-L1 is associated with self-tolerance of the immune system (Li et al., 2016).

The binding of receptor and ligand mediates the T-cell exhaustion as the cytotoxic functions of T-lymphocytes are downregulated. In local inflammation, this mechanism is relevant for preventing damage to the surrounding tissue. However, PD-L1 is also presented on the surface of tumor cells und can therefore be used by these cells to downregulate the host antitumor immune response. Due to this, the immune system is tricked into tolerating the tumor (Ancevski, Socinski & Villaruz, 2018).

Up to now, several monoclonal antibodies (mAbs) against PD-1 and PD-L1 are approved for clinical application. Nivolumab and pembrolizumab are used against PD-1 in NSCLC and metastatic melanoma, whereas durvalumab and atezolizumab target PD-L1. The latter two mAbs have demonstrated antitumor activity in many different types of cancer such as renal cell carcinoma, urothelial carcinoma, Hodgekin's lymphoma, hepatocellular carcinoma and head and neck cancer. However, an imbalance in the function of immune checkpoint molecules can lead to an uncontrolled immune response resulting in autoimmune side effects causing damage to normal organs and tissues (Naidoo et al., 2015).

In the case of NSCLC, pembrolizumab was granted accelerated approval in the US for the treatment of progressive disease during or after platinum-coupled chemotherapy (Herbst et al., 2016). According to Wang et al., 2019, the first approaches of coupling platinum-based chemotherapy with anti-PD-1 and anti-PD-L1 mAbs for the treatment of metastatic NSCLC without targetable mutations were made (Wang, Kulkarni & Salgia, 2019).

1.7 Chemotherapeutics

In this protocol, we examined whether combining cisplatin with different compounds such as AZD-7762, ML385, niclosamide, and others could potentiate the cytotoxic effects of this drug on permanent and primary NSCLC lines.

1.7.1 Cisplatin

Cisplatin was first described in 1845 but was not used as an antineoplastic agent before 1978. Since then, it is licensed worldwide as a therapeutic drug for head and neck, lung, colorectal and ovarian cancer. Carboplatin and oxaliplatin are two of many platinum-based derivates. The former has similar effects to cisplatin with the advantage of being less nephro- and neurotoxic as it has less side effects. Cisplatin has two *cis*-chloro groups, which are aquated intracellularly. This leads to a depletion of reducing equivalents in the cytosol and promotes oxidative stress (Galluzzi et al., 2014). Cisplatin forms covalent bonds with mitochondrial and nuclear DNA, preferentially by inducing DNA adducts with the nucleophilic N7 sites of purine bases. The most common form of cisplatin adducts are intrastrand complexes. These DNA adducts impair transcription and DNA synthesis and furthermore, result in cell cycle arrest. The cells try to repair the defect strands and, if the cisplatin-induced damage cannot be repaired, the cell undergoes apoptosis. However, the cells try to block the intracellular cisplatin cytotoxicity with several resistance mechanisms such as reduced uptake, increased efflux and induction of drug detoxification. Once cisplatin interacts with the DNA, the cells are forced to remove or tolerate the induced lesions (Rocha et al., 2018). Even though cisplatin has mild to moderate side effects, intrinsic and acquired drug resistance is one of the most notable problems in using this drug (Galluzzi et al., 2014).

1.8 Targeted therapy

1.8.1 Anti EGFR TKIs

As mentioned before, mutated EGFR is involved in synthesis and progression of different types of tumors and constitutes therefore an interesting target for therapy. In Figure 9 the course of treatment of EGFR mutated lung cancer can be seen. Anti-EGFR inhibitors include monoclonal antibodies or small molecule TKIs. First line TKIs, erlotinib and gefitinib, were developed in the early 2000s. They block the intracellular tyrosine kinase domain and inhibit the EGFR signaling pathway (Lee, 2017).

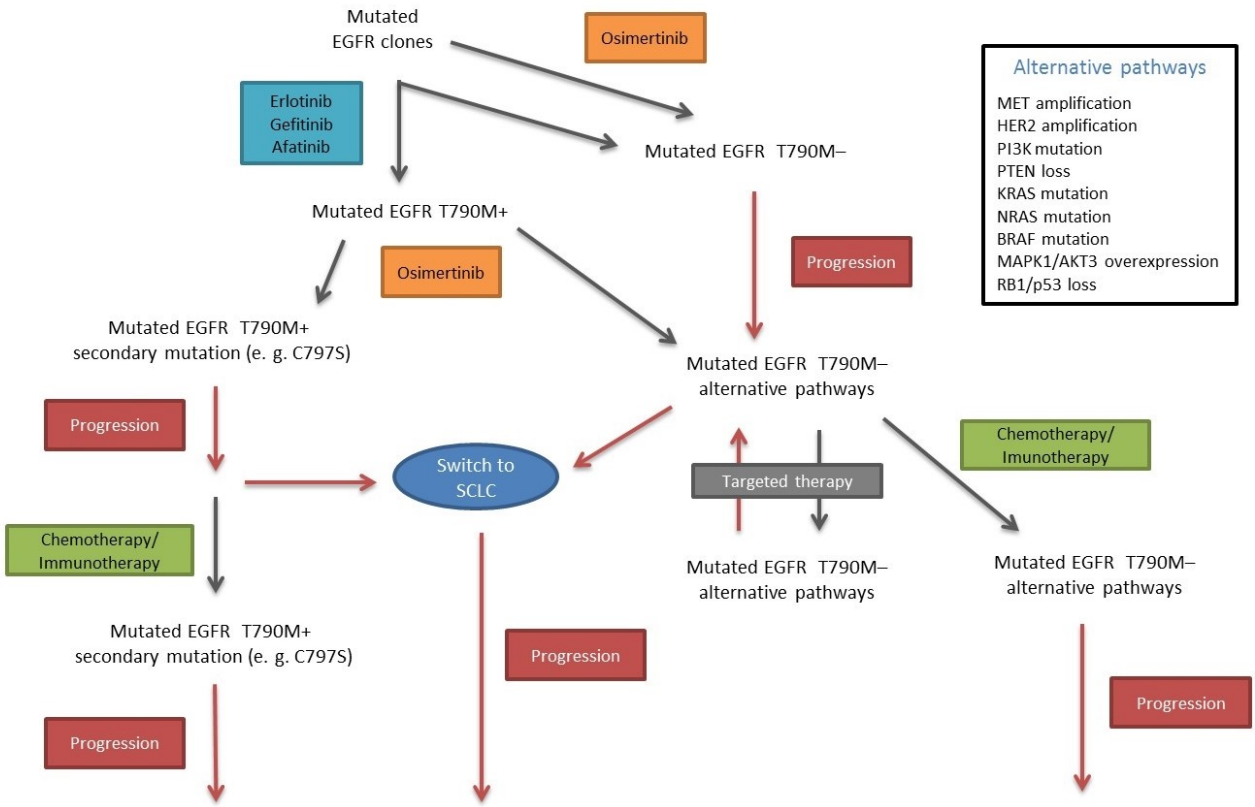

Figure 9 Course of treatment of EGFR mutated NSCLC.

However, patients treated with either erlotinib or gefitinib inevitably developed a resistance against these drugs. The median progression-free survival (PFS) is around 9-11 months after a treatment with either one of the TKIs. A point mutation (T790M) in exon 20 is responsible for this resistance. This mutation affects the ATP binding pocket on the cytoplasmatic tail end in the receptor and inhibits the binding of the TKIs to the receptor due to a steric hindrance (Lui et al., 2017). Afatinib, a TKI that irreversibly blocks all ErbB family members, can be used as a second-

line drug but it is primarily approved as a first-line drug against advanced NSCLC with squamous cell histology. This compound binds C797 covalently in EGFR at the lip of the binding site (Wind et al., 2016).

Finally, osimertinib is used as third line drug. This drug can overcome the T790M mutation in EGFR due to its different molecular scaffold. Osimertinib exhibited good response rates in clinical trials and is currently shifted to first-line use. However, the mutation C797S is a resistance mechanism of the tumor and leads to a relapse after the therapy with osimertinib (Lee, 2017).

1.8.2 Anti ALK TKIs

As mentioned above, ALK rearrangements account for about 5% of all AC incidences. In Figure 10 the course of an ALK mutated lung cancer is shown. Crizotinib has been used as a first line therapy drug as it shows a high clinical efficacy against ALK fusion-positive NSCLC. Most of the patients develop resistance against this drug within one or two years. However, crizotinib is unable to cross the blood brain barrier and has minimal activity against metastases in the central nervous system. Therefore, progressive patients on crizotinib often have brain metastases. After crizotinib failure alectinib is used as a second line therapy drug. It reveals a higher potency and also shows activity against L1196M which is the most common ALK mutation leading to crizotinib resistance. Additionally, alectinib can pass the blood brain barrier as it is not a substrate of P-glycoprotein with is a key efflux transporter for this barrier (Radaram et al., 2019; Wu, Savooji & Liu, 2016) Brigatinib and ceritinib are also second-line inhibitors of ALK. The first is a dual inhibitor of ALK and EGFR. It was originally formulated to counteract a broad spectrum of resistance mutations of ALK. Brigatinib also shows promising activity in the brain after crizotinib failure. Ceritinib on the

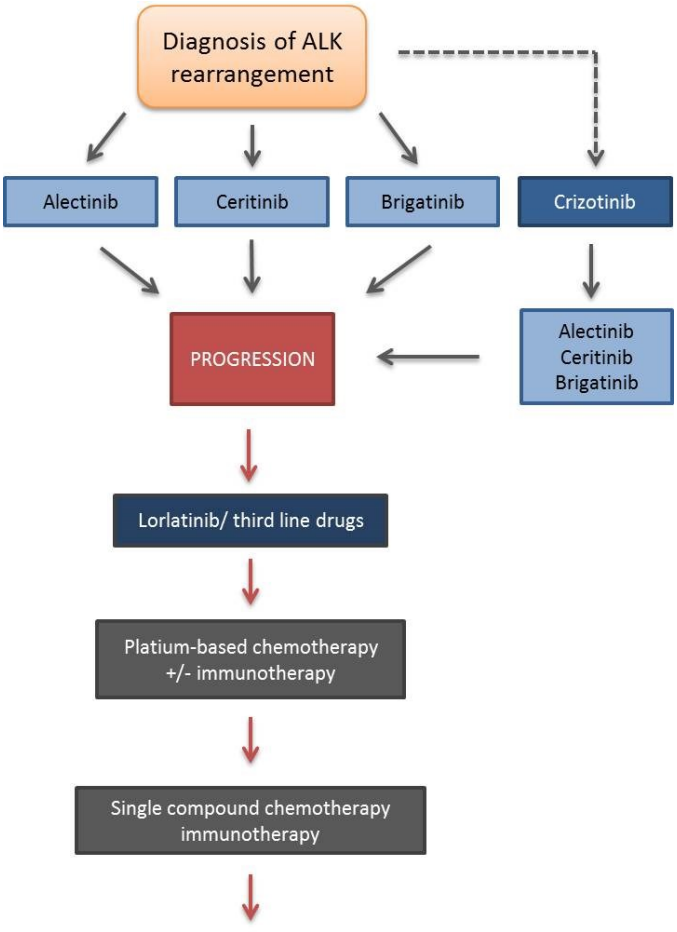

Figure 10 Treatment of ALK mutated lung cancer. Nowadays, Crizotinib is rarely used as first line drug as it promotes brain metastasis.

other hand inhibits IGF-1R and ROS1 and exhibits a higher activity against ALK and its most common mutations compared to crizotinib (Jain & Chen, 2017). Lorlatinib is then used as the third-line drug against ALK mutated lung cancer. It is a highly selective and potent drug which can pass the blood brain barrier. Additionally, lorlatinib inhibits ROS1 and its most common mutations. It seems to be an effective therapeutic option for ALK- and ROS1-positive patients (Shaw et al., 2017).

1.9 Modulators of cytotoxicity

1.9.1 AZD-7762

Checkpoint kinase 1 (Chk-1; serine/threonine kinase) is a critical element of DNA repair induced by cancer treatments or replicative stress. Normally, Chk-1 enables DDR in order to provide time for repair or, if unrepairable, to induce apoptosis. DDR is an important stress response which provides genomic stability and promotes DNA repair by activating cell-cycle checkpoints. Chk-1 is activated by ATR (Ataxia telangiectasia and Rad3 related protein) which results in cell-cycle arrest and destruction or sequestration of Cdc25 and prevents the inhibitory phosphorylation of cyclin-dependent kinases. Further, stalled replication forks are stabilized and proteins, which are crucial for DNA repair, are regulated via Chk-1. As a response to double strand breaks, Chk-2, also a serine/threonine kinase, is activated via ATM (ataxia telangiectasia mutated) which is a structural differential checkpoint kinase. However, Chk-2 also inactivates Cdc25.

AZD-7762 is an ATP-competitive CHK1/2 inhibitor and shows an increase of DNA damage by abrogating S and G2 checkpoints which results in increased tumor cell death. Studies have shown that Chk-1 inhibitors like AZD-7762 enhance the DNA damage induced by chemotherapeutics by overriding cell cycle arrest. Additionally, Chk-1 inhibitors are assumed to potentiate DNA-targeted chemotherapeutics *in vivo* and *in vitro* (Landau et al., 2012; Zabludoff et al., 2008).

1.9.2 Ganetespib

Ganetespib, also known as STA9090, is a small molecule heat shock protein 90 (HSP90) inhibitor. It is a second-generation resorcinol-based synthetic compound with wide clinical tolerability. HSP90 is an ATP-dependent molecular chaperone and one of the most commonly expressed proteins in cells. This protein is an essential component in protein folding, assembly and the degradation process of newly formed proteins. As a response to environmental influences and physiological incidences, HSP90 is overexpressed to ensure cell survival. In this function, HSP90

repeats cycles of client protein binding and controls the stability and activity of nascent client proteins. Because of its controlling properties, HSP90 is a promising target for cancer treatment as it stabilizes oncogenes which take part in important signaling pathways (Jhaveri & Modi, 2015).

1.9.3 ML385

ML385 is an inhibitor for the transcription factor nuclear factor erythroid 2-related factor 2 (Nrf2) by binding the domain that allows Nrf2 to heterodimerize. Normally, Nrf2 induces cytoprotective genes with antioxidant activity and in certain cancers like NSCLC Nrf2 is overexpressed as prosurvival mediator (Sigma Aldrich Co. LLC., 2019). Kelch-like ECH-associated protein 1 (KEAP1) regulates Nrf2 by directing proteasomal degradation. Therefore, a loss-of-function mutation of KEAP1 which often occurs in AC leads to a constitutive activation of Nrf2 signaling. Patients having mutations in Nrf2 and KEAP1 are also associated with decreased PFS (Singh et al., 2016). According to Singh et al., ML385 revealed specificity, selectivity and efficacy in combination with carboplatin in NSCLC in *in vivo* models.

1.9.4 Niclosamide

5-chloro-N-(2-chloro-4-nitro-phenyl)-2-hydrobenzamide, termed niclosamide, was originally used against human and animal infecting cestodes (Rajamuthiah et al., 2015). It inhibits oxidative phosphorylation, glucose uptake and anaerobic metabolism. In humans, this drug exhibits a maximal serum concentration of 0.25-6 µg/ml and displays antitumor toxicity even at low concentrations (Hamilton & Rath, 2017). By inhibition of Wnt/β-catenin signaling, niclosamide initiate cell cycle arrest, inhibition of growth and apoptosis. Additionally, niclosamide decrease the formation of primary and secondary tumorspheres in SCLC (Wang et al., 2018). Niclosamide was already successfully used in combination with cisplatin against cancer types such as breast, ovarian or prostate cancer *in vitro* (Hamilton & Rath, 2017).

1.9.5 Pristimerin

This compound is derived from plants of the *Celastraceae* and *Hippocrateaceae* family. It is also called 20α-3-hydroxy-2-oxo-24-nor-friedela-1-10,3,5,7-tetraen-carboxylic acid-29-methyl ester and it represents a quinonemethide triterpenoid (Li et al., 2019). Pristimerin demonstrated various pharmacological effects such as anticancer, anti-angiogenetic, anti-inflammatory, antiprotozoal and insecticidal properties. However, a main mode of action is not reported. This compound targets a variety of mechanisms including inhibition of NF-kB and AKT signaling pathway, cell cycle arrest induction, caspase activation and mitochondrial function (Zhang et al., 2019).

2 Patients and Methods

2.1 Cell lines and culture conditions

NSCLC cell lines BH295, BH438, BH495, BH593, BH611, BH615, BH659, BH686, BH725, BH738, BH748, BH751, BH773, BH802, BH827, BH833, BH840, BH888, BH918 and IVIC A were established previously in our lab from patients with NSCLC. An overview of patients with income date, gender, NSCLC stage, smoking history and mutations is shown in Table 1. Pleura collection and generation of cell lines was done after receiving informed consent according to the Ethics Approval 366/2003 of the Ethics Committee of the Medical University of Vienna, Vienna, Austria. The cell lines PC9, A549, H1299 and H1975 were purchased via ATCC (Manassas, Virginia, USA). Cells were cultured in RPMI-1640 medium (Seromed, Berlin, Germany) supplemented with 10% fetal bovine serum (Seromed) and penicillin/streptomycin antibiotics (Sigma-Aldrich, St. Louis, MO, USA) (Klameth et al., 2017). Adherent cell lines were split using trypsin (Sigma-Aldrich) two times/week and counted using the LUNA cell counter (Biozym, Vienna, Austria). All NSCLC cell lines grow adherent on the surface of cell culture flasks. In order to obtain 3D cultures, 10% agarose is poured into the bottom of the flasks and left to harden. The cells are then cultured as described above with the same medium in the coated flasks under cell culture conditions. Due to the negative charge of the agarose, the cells can not adhere to the bottom of the flask and may form 3D structures.

Table 1 Overview of the different pleura effusions and external purchased cell lines. py = pack years

patient	income date	gender	NSCLC stage	smoker	mutations
BH295	12.04.2017	-			ALK+
BH438	-	-			
BH495	11.04.2018	M	progression after afatinib		
BH593	30.08.2018	F	primum	Ex (30 py)	
BH611	16.09.2018	M	suspected lung cancer	smoker (40py)	N-ras
BH615	19.09.2018	F	progression after osimertinib	Non-smoker	EGFR
BH659	05.11.2018	F	progression after afatinib & osimertinib, SCLC transformation	non-smoker	EGFR Del19, T790M+
BH686	23.11.2018	F	continuation of treatment with osimertinib, SCLC transformation, same patient as BH659		EGFR Del19, T790M+
BH725	08.01.2019	M	primum; high tumorload		
BH738	23.01.2019	F	suspected lung cancer; high tumorload		
BH748	30.01.2019	F	primum		
BH751	31.01.2019	F	progression, afatinib, osimertinib, crizotinib, high tumorload, SCLC transformation		
BH773	25.02.2019	M	suspected lung cancer		
BH802	13.03.2019	F	progressive lung cancer		
BH827	10.04.2019	M	primum, Cluster, brigatinib		ALK+
BH833	12.04.2019	M	suspected lung cancer		
BH840	16.04.2019	F	progression under afatinib		EGFR Del19
BH888	09.07.2019	M	suspected lung cancer; forming cluster		
BH918	28.08.2019	M	progressive lung cancer		
IVIC A	23.08.2016	F	osimertinib, SCLC transformation		
external purchased cell lines					
H1299	-	M	derived from metastatic site: lymph node		
H1975	-	F	adenocarcinoma		
A549	-	M	Lung; epithelial		
PC9	-	M	adenocarcinoma; derived from metastatic site: lymph node		

2.2 Cell proliferation assays

1 x 10^4 cells in 100 µl medium were distributed to wells of 96-well microtiter plates (TPP, Trasadingen, Switzerland) and ten 2-fold dilutions of the test compounds were added in triplicate. Assays were performed at least in triplicate. The plates were incubated for four days under tissue culture conditions and viable cells were detected using a modified MTT assay (EZ4U, Biomedica, Vienna, Austria). IC_{50} values were determined from dose-response curves using Origin 9.1 software (OriginLab, Northampton, MA, USA).

2.3 Human Phospho-Kinase Array

The phosphorylation profiles of kinases (ARY003B) were tested using the Proteome Profiler™ Array (R&D System, Inc., Minneapolis, USA). The samples were prepared according to the instruction manual attached to the kit. All cell lines used in this array were pretreated with cisplatin and compared to untreated controls. The cell lines BH659 and BH686 were each treated with 20 nM of cisplatin for three days due to high chemosensitivity. After this incubation, the cells were washed and used for the array. H1975, BH495, BH611 and BH802 were pretreated with 3 µM cisplatin as these cell lines are more resistant to the drug compared to others. The experiments were done in duplicate. The cells are solubilized at 1 x 10^7 cells/ml with a lysis buffer and are rocked at 2-8°C for 30 min. After preparing the required reagents and samples, two membranes (A&B) which have catcher antibodies immobilized on them, are incubated with an array buffer for one hour to block the membranes. Subsequently, the buffer is aspirated and the membranes are incubated with the prepared samples overnight at 2-8 °C on a rocking platform shaker. All other working steps can be done at room temperature.

Next, the membranes are washed with wash buffer for 10 minutes with a total of three washes. Specific targets were identified with a cocktail of biotinylated detection antibodies, followed by streptavidin-HRP and a chemiluminescent reagent. After recording the signals using the ChemiDoc™ Imaging System (BioRad, Hercules, CA, USA), the capture spots which correspond to the amount of protein were analyzed using ImageJ (NIH, Bethesda, MD, USA) and ORIGIN 9.0 software (OriginLab, Northampton, MA, USA). Calibration within the membranes was done using the six control spots provided.

2.4 Chou-Talalay method

Based on the *The Median-Effect Plot* and *CI algorithms*, a plot of CI values at different effect levels (fa's) can be determined by computer simulation (e.g. CompuSyn). Entering a series of "dose (D) and effect (fa)" into computer for each drug alone and their combinations, the software will automatically simulate the CI values at different fa levels based on the CI algorithm. This plot is also called the Fa-CI plot or the Chou-Talalay plot (Chou, 2010). Depending on the experimental design, the combination relations can be at constant ratio or at non-constant ratios. In combination plots an index value of 1 indicates an additive effect, whereas combination indices below and exceeding this value point to synergism and antagonism, respectively.

2.5 Gene expression analysis

This part of the experiment was performed with the kind support and cooperation of Dr. Eva Obermayr, Department of Gynecology, Medical University of Vienna.

Total RNA was extracted from the cell lysates using the RNeasy Micro Kit (Qiagen, Hilden, Germany) without DNase treatment. The total amount of RNA was converted into cDNA using the SuperScript VILO Mastermix (Invitrogen, Carlsbad, CA). qPCR was done in duplicates in a 10µl total reaction volume on the ViiA7 Real-Time PCR System using the TaqMan® Universal Mastermix II and exon spanning TaqMan® assays specific for EpCAM, NCAM1, CHGA, SYP, ENO2, and CDKN1B (Life Technologies, Carlsbad, CA) with default thermal cycling parameters (50° C 2 mins; 95° C 10 mins; 40 cycles at 95° C 15 s, 60° C 1 min). A qPCR specific for CK19 was performed at 65°C annealing/extension with forward and reverse primers which correspond to published primer sequences and with a FAM labeled hydrolysis probe (5'-TgTCCTgCAgATCgACAACgCCC-3´) (Stathopoulou et al., 2003). Raw data were analyzed using the ViiA7 Software v1.1 with automatic threshold setting and baseline correction. If the fluorescent signal did not reach the threshold in both duplicate reactions, the sample was regarded as negative (Obermayr et al., 2019).

2.6 Analysis of PD-L1 expression

Cells were split using trypsin (Sigma-Aldrich). 1 x 10^6 cells were suspended in 100 µl PBS (Lonza™, Basel, Switzerland) and incubated with PE anti-human CD274 (B7-H1, PD-L1) antibody (BioLegend®, San Diego, CA) overnight at 4 °C. As a conjugate Anti-Mouse IgG (whole molecule)–FITC antibody produced in goat (Sigma-Aldrich) was used. The cells were washed in between every step. For each cell line (H1975, H1299, PC9, BH495, BH751 and BH888) a conjugate control and a sample incubated with the anti-human CD274 antibody were prepared. 10 µl of the cell suspension was applied to a specimen slide and coated with a cover glass. Photos were taken with the CC-12 camera on an Olympus BX50 Fluorescence microscope (Olympus, Hamburg, Germany) with 200x magnification and evaluated via the cell^P professional imaging software (Olympus). According to Chen et al., H1975 showed a high mRNA level of PD-L1 and was therefore used as a positive control. As a negative control H1299 was used as this cell line showed minor to negative expression of PD-L1 (Feng et al., 2017).

2.7 Statistical Tests

In the present work, representative results from at least three independent experiments are shown. The numerical data is presented as the mean ± standard deviation (SD) of the mean. Statistical significance was tested by Student's t-test and p-value < 0.05 is regarded as significant difference.

3 Results

3.1 Analysis of PD-L1 expression

In order to determine the PD-L1 expression of the different cell lines, they were stained with FITC anti-human CD274. For every cell line an additional conjugate control was made. As for positive control H1975 and as negative control the cell line H1299 was used and both showed the expected results.

Cell line BH495 exhibited no expression of PD-L1 (Figure 11A). Cell line BH751 (Figure 11B) revealed minor expression of PD-L1 and PC9 also yielded PD-L1 expression (not shown). The testing with BH888 failed as this cell line showed a positive staining in the conjugate control. The positive expression of PD-L1 on cell line H1975 is shown in Figure 11C. As a result, the testing for PD-L1 was stopped as only BH751 showed an appropriate PD-L1 expression. Accordingly, the clinical data of the patients recorded no significant expression of PD-L1 at diagnosis of the NSCLC in the beginning.

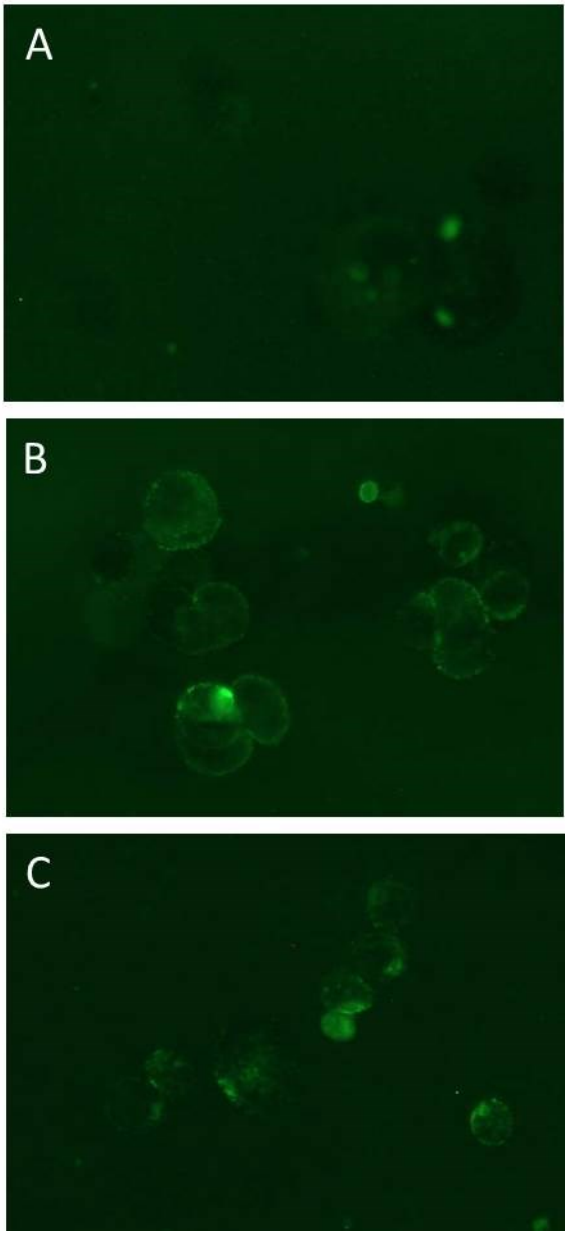

Figure 11 A) section of the microscope picture of cell line BH495. This cell line showed no expression of PD-L1. B) section of the microscope picture of cell line BH751. C) section of the picture of cell line H1975. All three pictures were taken with a magnification of 200.

3.2 2D cultures

3.2.1 Cisplatin cytotoxicity

Next, we checked the chemosensitivity of cisplatin on the different cell lines. In Figure 12 four different dose response curves for cisplatin are shown. BH495, BH827 and H1975 yielded a higher resistance against cisplatin compared to BH659. The latter cell line represents a NSCLC to SCLC transformed line and is particularly sensitive to cisplatin.

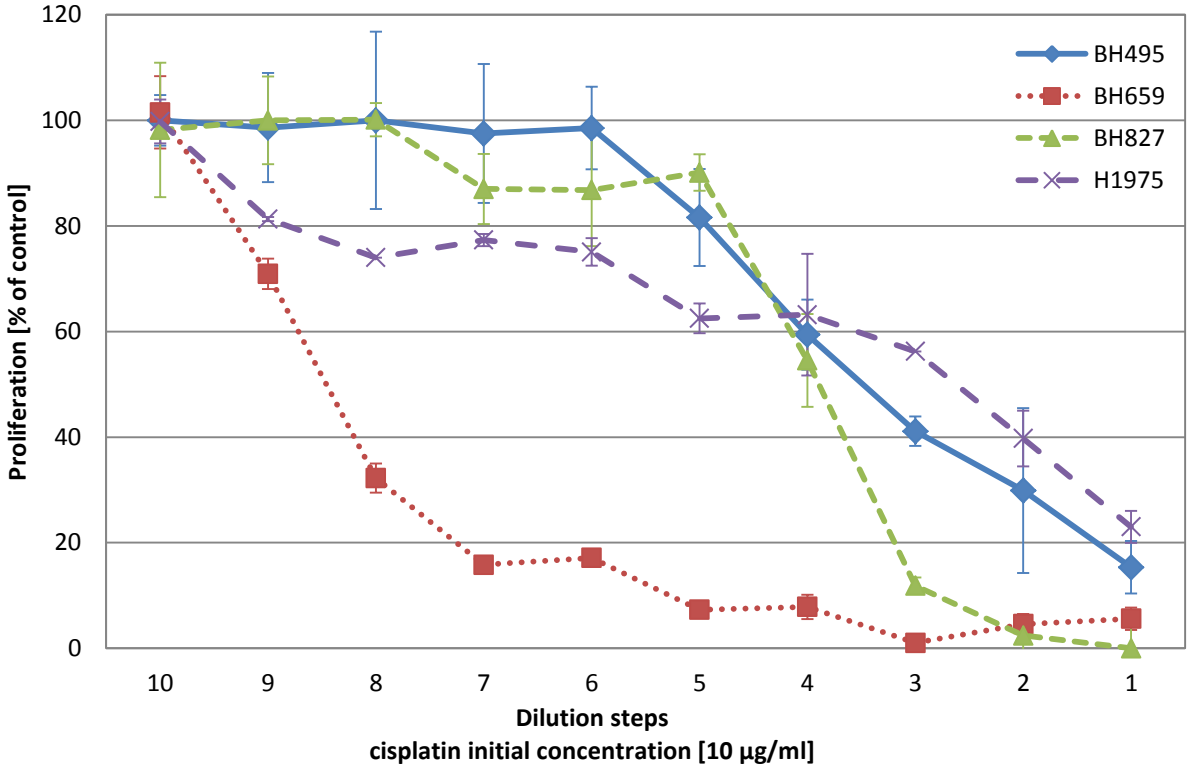

Figure 12 Cytotoxicity of cisplatin against the cell lines BH495, BH659, BH827 and H1975.

In order to identify the cytotoxic effect of cisplatin on the various cell lines, the IC_{50} for each cell line was calculated from dose-response curves of cytotoxicity tests. At least three individual tests were used to compute the respective value for each cell line. The IC_{50} values of the various cell lines are shown in Figure 13. The most resistant cell line against cisplatin is BH438 which showed an IC_{50} of 9.45 ± 2.53 µg/ml. BH659 and BH686, two samples from the same patient taken 18 days apart of each other, yielded the highest sensitivity against cisplatin as their IC_{50} values are 0.05 ± 0.02 and 0.08 ± 0.05 µg/ml, respectively. All other cell lines are in between this range of IC_{50} values. There was no significant difference in the sensitivity of the pleural cell lines and permanent cell lines (mean pleural cell lines: 3.64 ± 2.35 µg/ml; mean permanent cell lines: 2.89 ± 1.28 µg/ml; p-value = 0.5484).

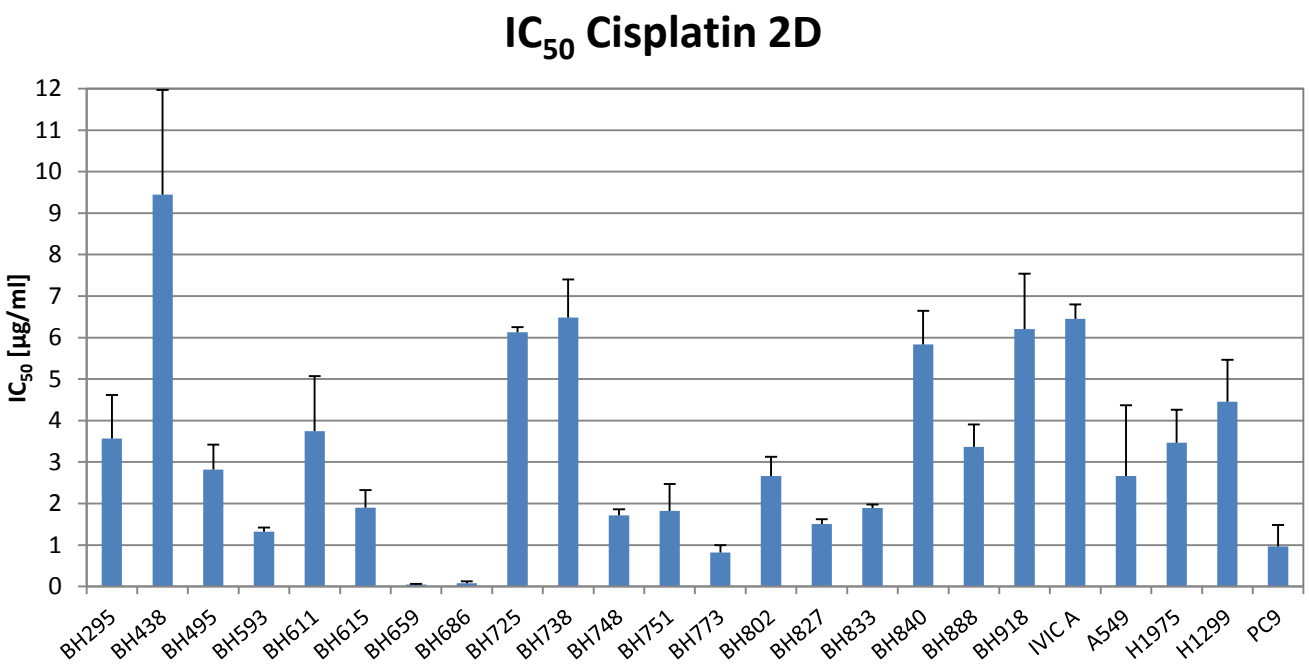

Figure 13 IC_{50} values of the different cell lines treated with cisplatin. Data are shown as mean values ± SD.

3.2.2 Cisplatin & modulator combinations

3.2.2.1 Cisplatin & Chk1/2 inhibitor combination

The first compound tested was AZD-7762, a Chk1/2 inhibitor. In Figure 14 a dose response curve of cell line BH751 treated with cisplatin, AZD-7762 and the combination of both drugs is shown. From this curve a CI-value could be determined.

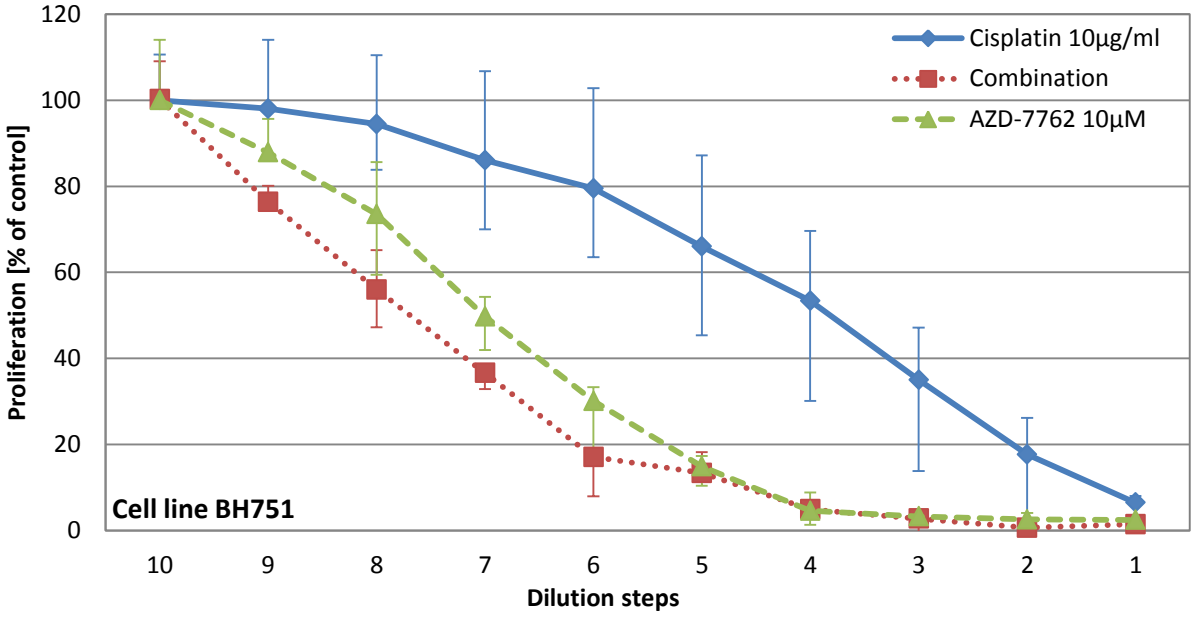

Figure 14 Dose response curve of a combination of cisplatin and AZD-7762 for cell line BH751.

A CI-value below 1 indicates a synergism between two compounds on a cell line. The smaller the value the greater is the synergism between the used compounds. A value of 1 points to an additive effect of the drugs on the cell line. A value exceeding 1 indicates an antagonistic effect and the cytotoxic effect of the combination of two drugs is lower than that of the individual compounds alone. In this case, a treatment with the more efficient compound should be considered.

In Figure 15 the CI-values of the cisplatin/AZD-7762 combinations are shown. The cell lines BH611, BH659, BH827, BH888 and PC9 revealed a greater CI than 1. The effect of the combination can therefore be considered as antagonistic. BH918, H1975 and A549 yielded a CI around 1. The combination has an additive effect on the cell lines. The remaining cell lines listed show a CI below 1. In these cases, a treatment with the combination of cisplatin and AZD-7762 would be more efficient compared with a treatment with each one of the compounds.

For a comparison of the results, a significance test for the cell lines was done which showed a synergism when treated with this combination between primary and permanent cell lines. This difference gave a p-value of 0.0018 and can be considered as statistically significant (mean of primary cell lines: 0.48 ± 0.16; n = 10; mean of permanent cell lines: 0.98 ± 0.32, n = 4). The same calculation was done for antagonistic effects between primary and permanent cell lines. This yielded a p-value of 0.0809 which cannot be counted as statistically significant (mean of primary cell lines: 2.60 ± 1.57, n = 6; mean of permanent cell lines: 0.98 ± 0.32, n = 4).

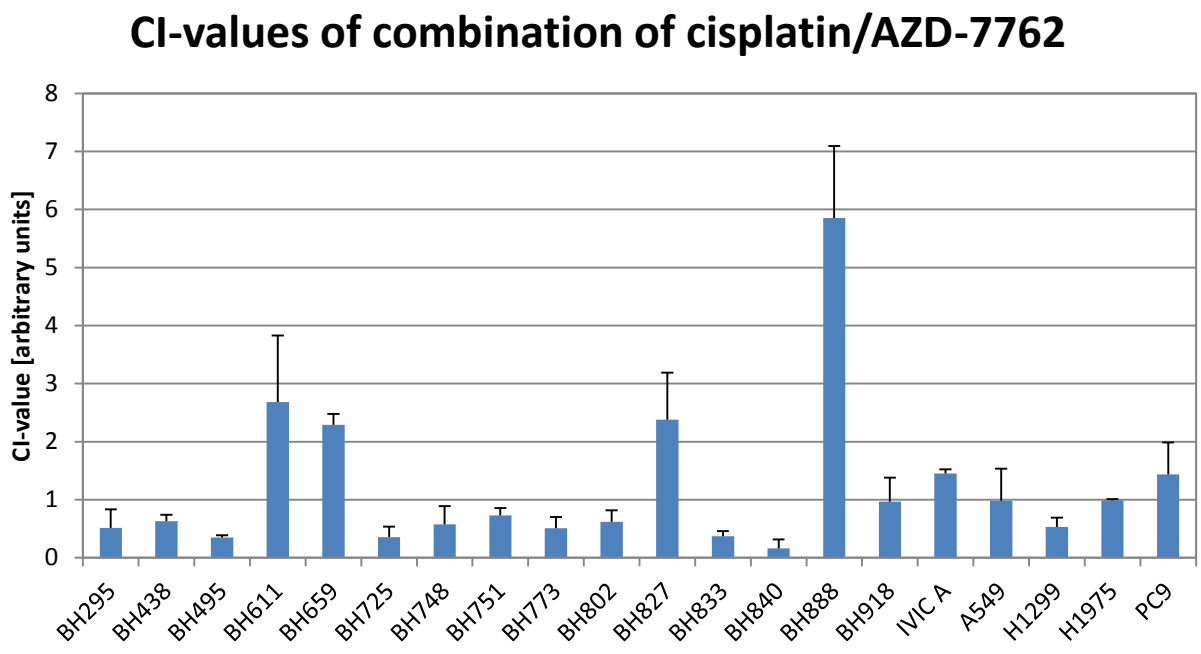

Figure 15 Bar graph showing the CI-values of the combination of cisplatin and AZD-7762 on the different cell lines. Data are shown as mean values ± SD.

3.2.2.2 Cisplatin & HSP90 inhibitor combination

The next compound tested was STA9090. The combination of cisplatin and STA9090 revealed a synergism in only two cell lines, namely BH773 and BH833 (Figure 16). Accordingly, the remaining cell lines yielded a value higher than 1. BH611, not shown in the bar graph, revealed a very high antagonistic effect compared to the other cell lines. Furthermore, the permanent cell lines showed an antagonistic effect when treated with this combination.

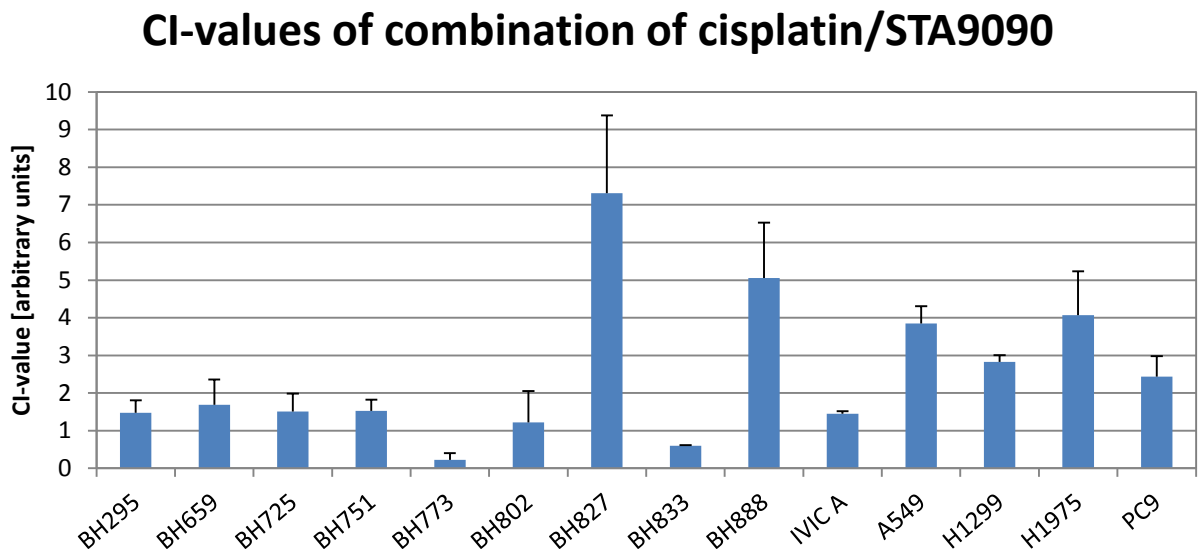

Figure 16 CI-values of the various cell lines treated with a combination of cisplatin and STA9090. Data are shown as mean values ± SD.

3.2.2.3 Cisplatin & Nrf2 inhibitor combination

Next, the cell lines were treated with a combination of cisplatin and ML385, an Nrf2 inhibitor. In Figure 17 the different cell lines and the corresponding CI-values are listed. H1299 was the only cell line which showed a synergism with these compounds. BH611 showed an additive effect upon treatment with this combination while the remaining cell lines revealed a marked antagonistic effect. BH295 and BH827 are not shown in the bar graph as these cell lines showed exceedingly large CI-values.

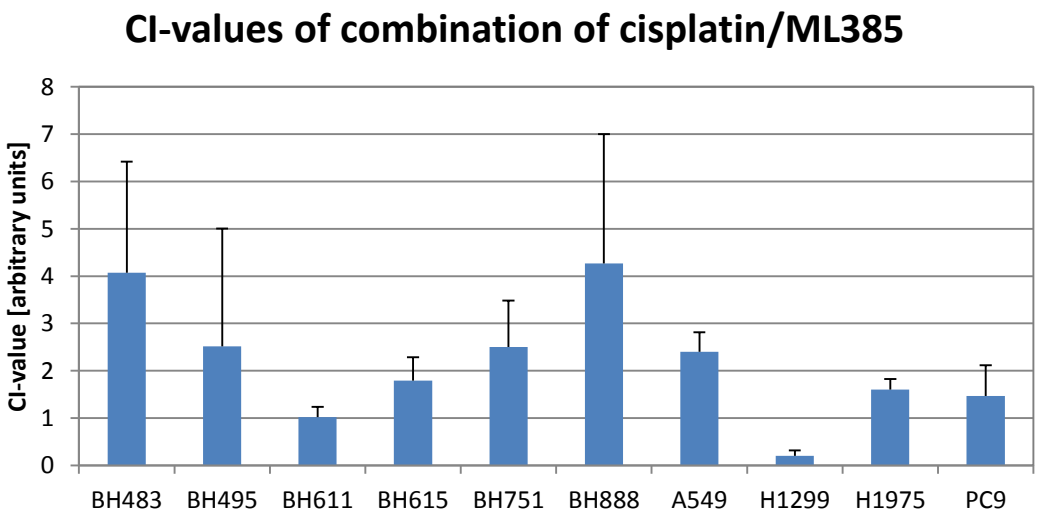

Figure 17 CI-values of the cell lines treated with a combination of cisplatin and ML385. Data are shown as mean values ± SD.

3.2.2.4 Cisplatin & niclosamide combination

The combination of cisplatin and niclosamide yielded lower CI-values compared to the other modulators tested (Figure 18). BH593, BH751 and BH773 showed an antagonistic effect with the combined drugs. BH802 revealed an additive effect and the remaining cell lines yielded a synergistic effect. The combination effectuated the highest synergism in A549 (CI-value of 0.007 ± 0.003) among the permanent cell lines and in BH611 (CI-value of 0.234 ± 0.056) for the pleural lines. Apparently, the combination of these two compounds yielded no significant differential impact on the permanent cell lines compared to the pleural cell lines. However, it showed significance on the effect of antagonism and synergism upon all the cell lines tested (mean antagonistic cell lines: 2.62 ± 1.57; mean synergistic cell lines: 0.44 ± 0.25; p-value: 0.0001).

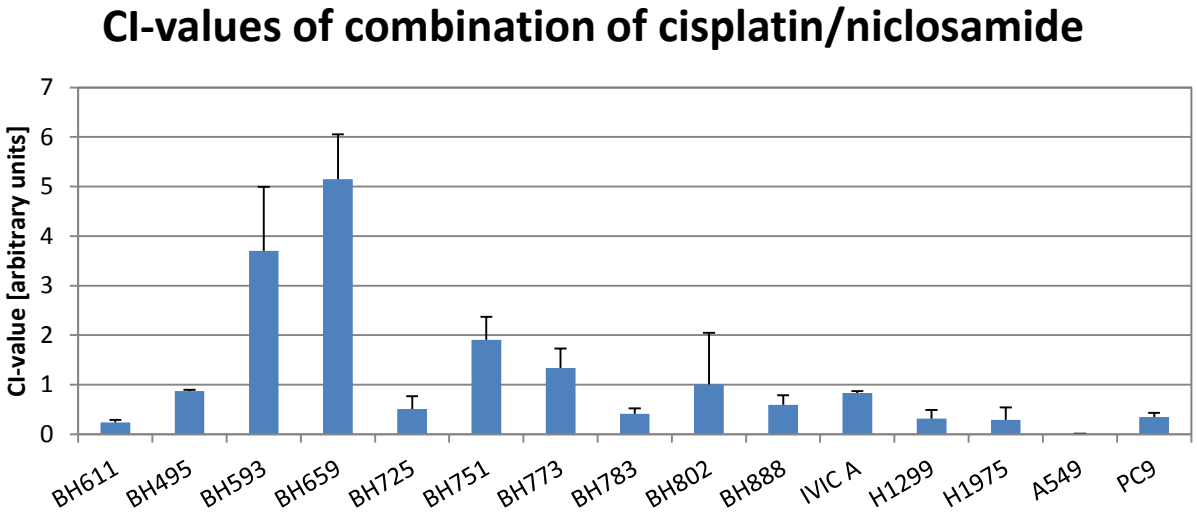

Figure 18 Bar graph showing the different CI-values of the various cell lines. Data are shown as mean values ± SD.

3.2.2.5 Cisplatin & pristimerin combination

Combining cisplatin and pristimerin showed a synergistic effect in BH751, BH888, H1299 and H1975 cell lines (Figure 19). BH773 yielded an additive effect when treated with this combination. BH827 and PC9 and BH611 (data not shown) revealed an antagonistic effect.

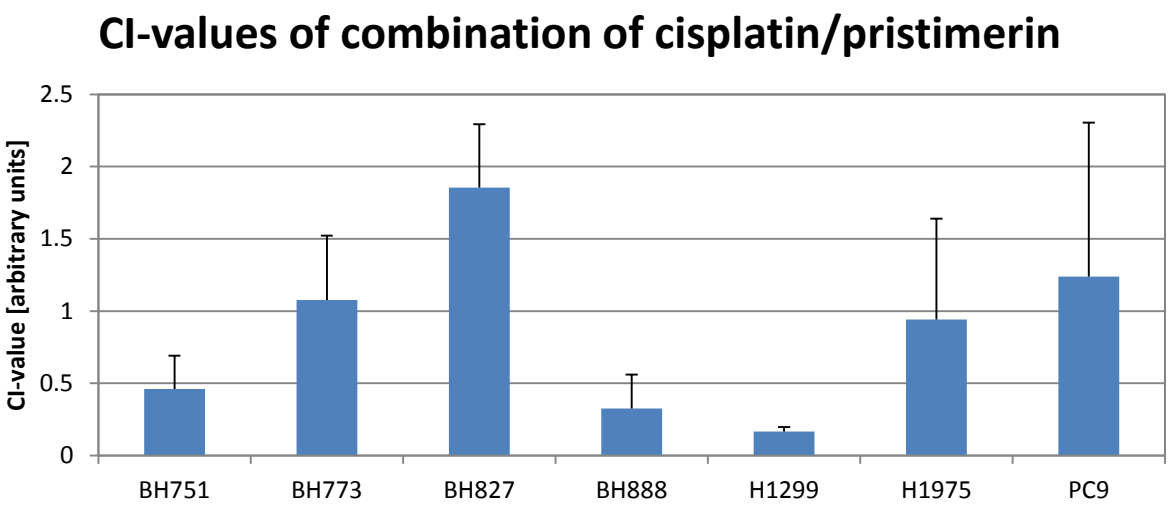

Figure 19 CI values of the combination of cisplatin and pristimerin on the different cell lines. Data are shown as mean values ± SD.

3.3 3D cultures of NSCLC cell lines

In order to obtain 3D cultures from 2D ones, the cell lines were cultivated on agarose-coated culture flasks. Figure 20 depicts a direct optical comparison of IVIC A. Although most of the cells in 2D culture grow attached on the bottom of the flask some of them appear to grow lightly detached which is indicated by the white border of the cells (A). On an agarose layer, this cell line tends to form tighter packed 3D structures (B). BH888, BH751 and BH659 also formed 3D cultures within a few days but these cellular aggregates tend to be more loosely. BH686 was not cultured on agarose-coated flasks as BH659 is from the same patient. However, not all of the cell lines could be forced to grow in 3D: both BH725 and BH611 failed to do so. A549, H1299 and H1975 were used as permanent control cell lines.

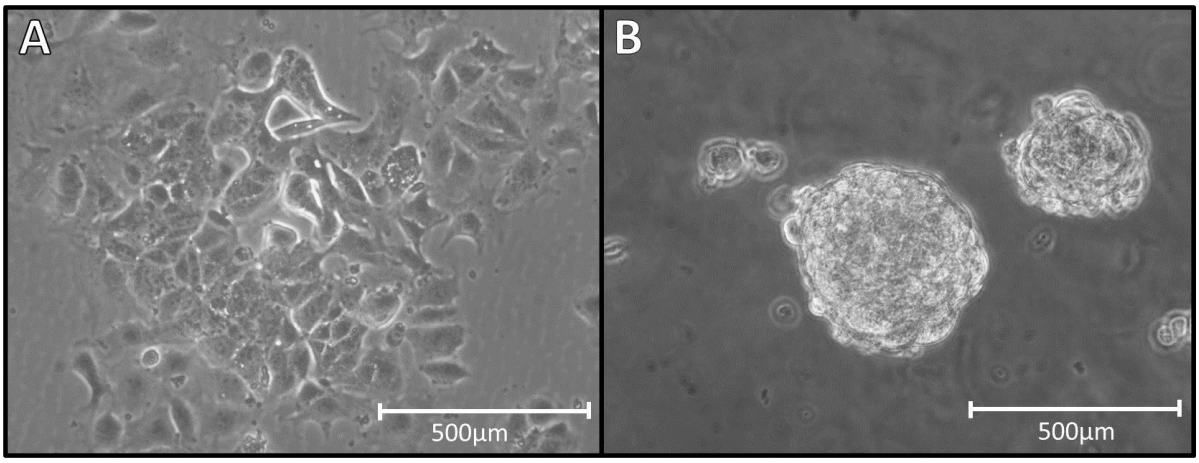

Figure 20 comparison of cell line IVIC A. A) image of adherent cells. B) same cell line cultured in 3D on 10% agarose.

3.3.1 Cisplatin-sensitivity of lung cancer lines in 3D culture

In order to determine the effect of the cytotoxic drug cisplatin, we calculated the IC_{50} values of this chemotherapeutic in 3D cultures and compared the values to those of the 2D cultured cells. BH888, BH751 and H1975 showed a higher sensitivity to cisplatin in 2D than in 3D. However, BH495, A549 and H1299 were more resistant to cisplatin when cultured in 3D. The clusters of A549 and H1299 yielded the highest IC_{50} values with 7.22 ± 1.64 and 7.04 ± 1.35 µg/ml, respectively. In contrast, the 2D cultures of the same cell lines exhibited 4.45 ± 1.01 µg/ml for H1299 and 2.67 ± 1.70 µg/ml for A549. These two pairs of IC_{50} values accounted for a p-value of 0.0381 for H1299 and 0.0254 for A549, respectively and therefore, can be considered as statistically significant (Figure 21). The two values for BH495 yielded a p = 0.0461 and can be

considered as significant. The 3D culture of BH751 was more sensitive to cisplatin compared to 2D. The difference of these two values also showed significance (p = 0.0453).

On the other hand, the 3D cultures of BH888 and H1975 were more sensitive to cisplatin compared to the 2D ones. Although cell lines such as BH888 exhibited an IC_{50} value of 3.37 ± 0.54 µg/ml in 2D and 2.92 ± 0.14 µg/ml in 3D and H1975 showed an IC50 of 3.47 ± 0.79 µg/ml for the adherent culture and 1.88 ± 0.63 µg/ml for the 3D culture this tendency proved to not be statistically significant.

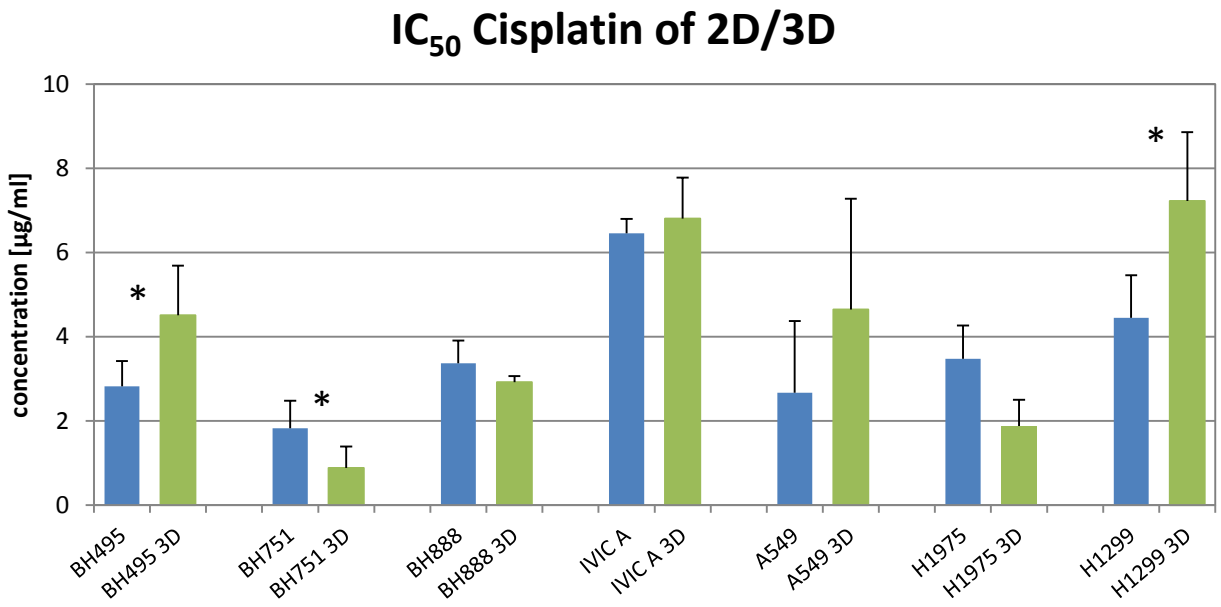

Figure 21 bar graph showing IC_{50} values of cisplatin exhibited by permanent and primary NSCLC cell lines compared to the 3D cultured of the same cell lines. Data are shown as mean values ± SD. Statistical significance is indicated by *.

3.3.2 Cisplatin combinations in 3D cultures

Next, the CI values for the different modulators were compared. Each modulator was tested for the 2D cultured cells and the 3D ones. Against H1299 3D the combination of cisplatin and AZD-7762 appears to have the highest cytotoxicity as the CI Value is 0.0003 ± 0.0001. This indicates a high synergism of the combination of the two compounds on this cell line. A549 and BH888 in 3D cultured showed an additive effect of the drug combination as the CI is around 1. However, the two CI values of A549 in 2D and 3D are very similar, therefore excluding an influence of the cellular aggregation in this case. There was also no significant difference of BH659 in 2D and 3D when treated with the combination. IVIC A and H1975 in 3D showed a significant antagonism when treated with cisplatin/AZD-7762. The bar graph of the CI values of the combination of cisplatin and AZD-7762 is shown in Figure 22.

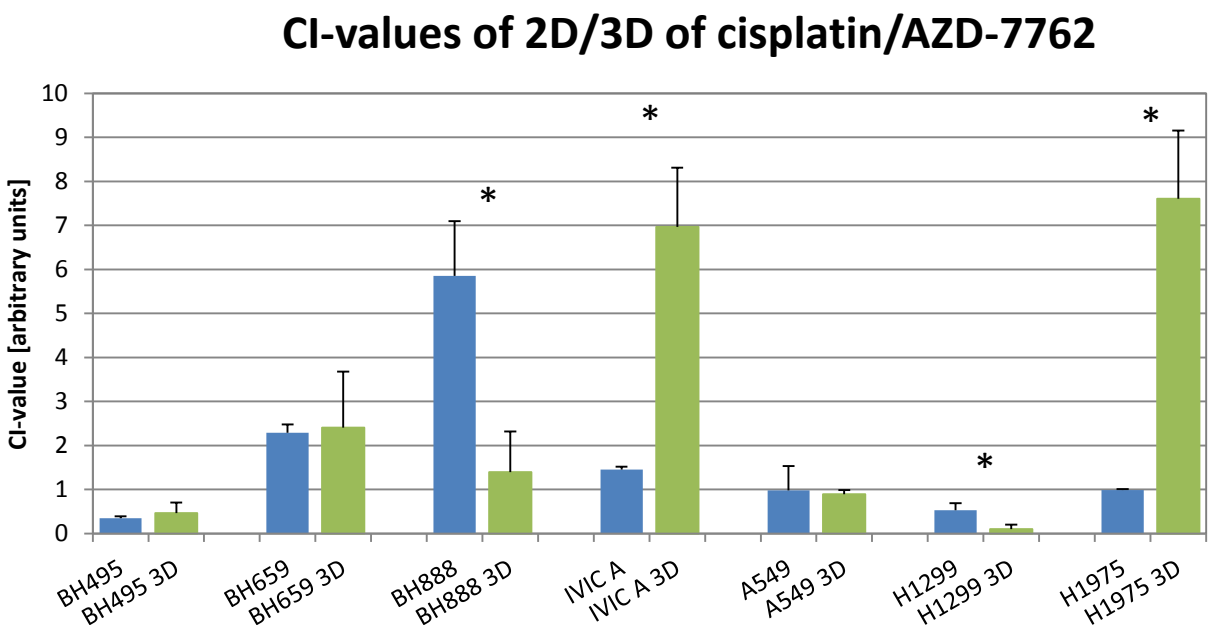

Figure 22 bar graph showing the CI values for the compound AZD-7762 for both the 2D and 3D cultures. Data are shown as mean values ± SD. Statistical significance is indicated by *.

In Figure 23 the CI values for both the 2D and 3D cultures for the modulator STA9090/cisplatin combination are shown. H1299, H1975, A549, IVIC A and BH888 showed a lower CI value in 3D compared to 2D. However, H1299 and IVIC A yielded a CI below 1 in 3D which indicates synergism between cisplatin and STA9090. Against cell line A549 3D the combination of cisplatin and STA9090 showed an additive effect. BH751 showed a significant higher CI in 3D compared to 2D indicating antagonism. All of the pairs can be considered significantly different except for BH888 and BH659.

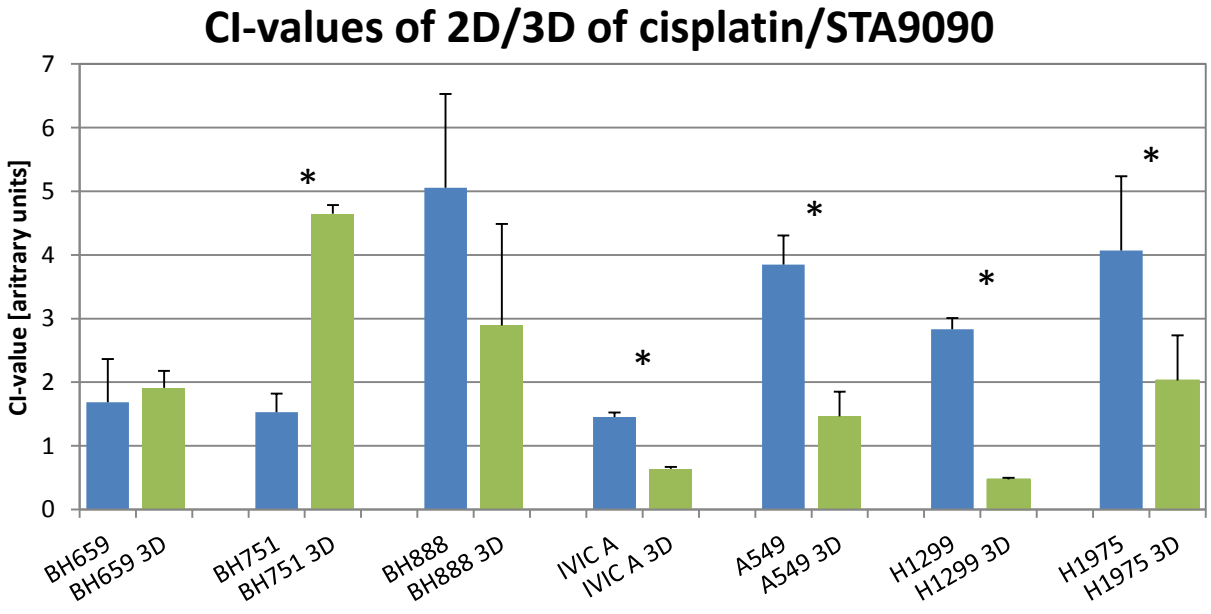

Figure 23 comparison of CI values of STA9090 for the different cell lines in 2D and 3D. Data are shown as mean values ± SD. Statistical significance is indicated by *.

The CI-values for the activity of the combination of niclosamide and cisplatin against the cell lines BH751, A549, H1299 and H1975 in 3D were higher compared to those of the corresponding 2D cell lines but this combination still lies in the synergistic range of CIs. The value of A549 2D is 0.007 (Figure 24). BH751 and BH659 showed no synergistic or additive effect in both types of cell cultivation methods. In case of BH495 no significant difference was detectable.

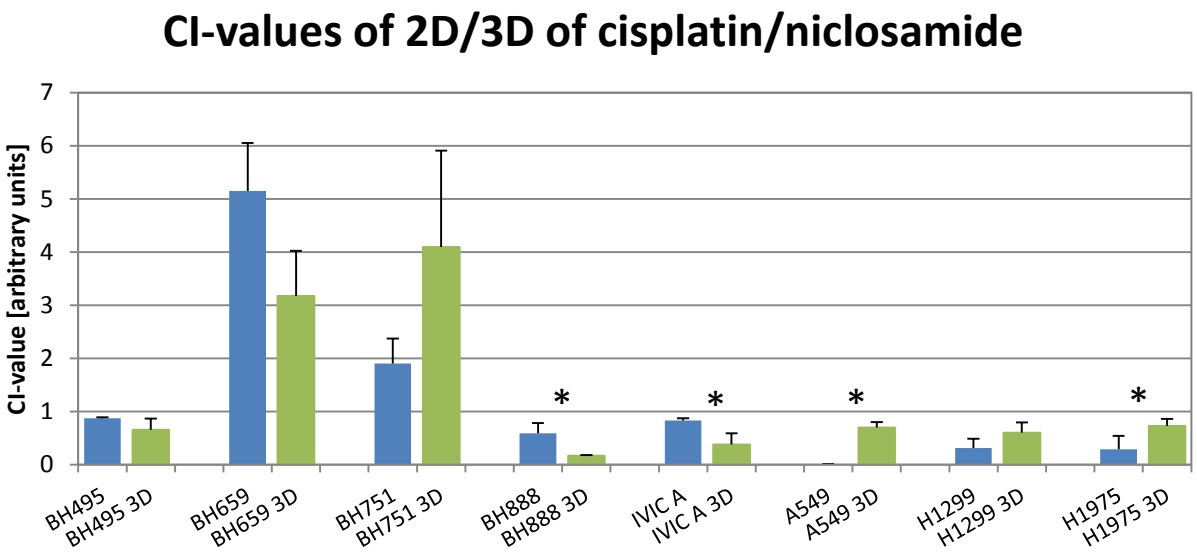

Figure 24 comparison of the CI values for the different cell lines in 2D and 3D for the modulator niclosamide. Data are shown as mean values ± SD. Statistical significance is indicated by *.

In Table 2 the comparisons of the CI-values for 2D and 3D for cell line BH888 for the combination of cisplatin with either ML385 or pristimerin are shown. The combination of ML385 and cisplatin yielded in both variants of cell cultivation of BH888 an antagonistic effect. However, cisplatin combined with pristimerin in BH888 in 2D showed a highly synergistic effect and in 3D an antagonistic effect. This comparison is also statistically significant with p = 0.0003.

Table 2 Overview of the CI-values of BH888 in 2D and 3D for the combination of either ML385 and cisplatin and pristimerin and cisplatin.

Cell line	CI-value	±SD	p-value
ML385			
BH888	4.27	2.73	0.2666
BH888 3D	2.03	1.06	
pristimerin			
BH888	0.32	0.24	0.0003
BH888 3D	4.64	0.99	

3.4 Human phosphokinase array

Next, the different phosphorylation profiles of kinases of six different cell lines were compared. Cisplatin treated and control groups of H1975, BH495, BH802, BH611, BH659 and BH686 were analyzed by human phosphokinase arrays. The complete list of all arrays can be found in the appendix. For this thesis, only the most significant six proteins of the arrays were chosen.

Chk-2, a serine/threonine kinase, showed a higher phosphorylation in the cisplatin treated groups of H1975, BH495, BH659 and BH686 (Figure 25). BH686 showed a significantly lower phosphorylation in the control group compared to BH659. Generally, the difference of phosphorylation between the two groups of BH686 is higher compared to BH659. BH611 yielded no differential phosphorylation of this protein between both groups. The control group of BH802 revealed a higher phosphorylation of Chk-2 than the cisplatin treated one.

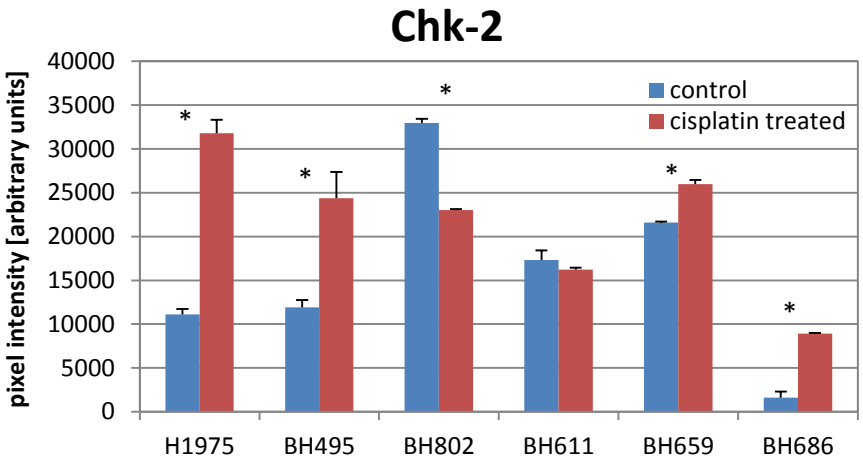

Figure 25 Comparison of the phosphorylation profile of Chk-2 (T68). Data are shown as mean values ± SD. Statistical significance is indicated by *.

Next, ERK1/2 with T202/Y204 and T185/Y187 phosphorylation sites was analyzed for the different cell lines as shown in Figure 26. The alteration in the phosphorylation of the two groups of H1975, BH802 and BH659 revealed no significant difference, most likely because ERK1/2 in these cell lines is hyperphosphorylated from the outset. Apparently, the treatment with cisplatin had no significant impact on the phosphorylation of this protein. However, BH495, BH611 and BH686 revealed a hyperphosphorylation of ERK1/2 in the cisplatin treated group. BH611 showed the biggest difference compared to all other cell lines. The difference in phosphorylation in BH686 was again significantly lower compared to the other cell lines.

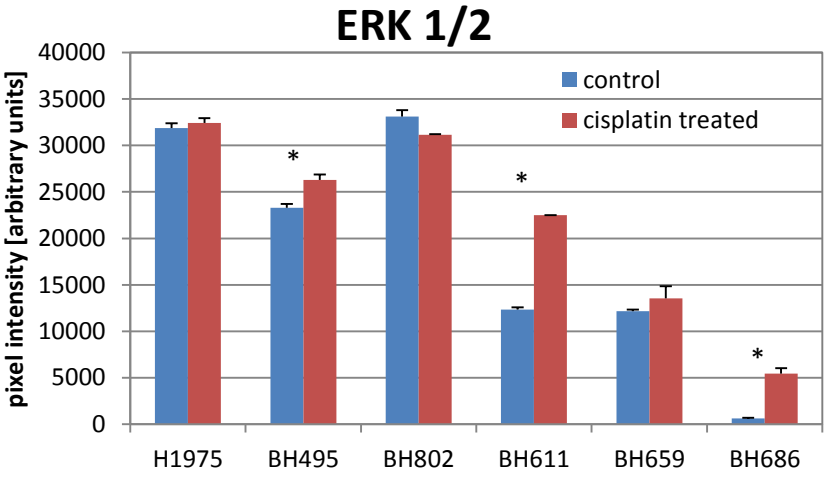

Figure 26 Comparison of the phosphorylation profile of ERK1/2 (T202/Y204, T185/Y187). Data are shown as mean values ± SD. Statistical significance is indicated by *.

The alteration of the serine-threonine kinase AKT1/2/3 with the phosphorylation site T308 was limited to H1975 and BH686 (Figure 27). BH495, BH802 and BH659 revealed a high basal phosphorylation in contrast to BH611; however, all differences for the cisplatin treatment were not significant. BH611 showed the lowest phosphorylation.

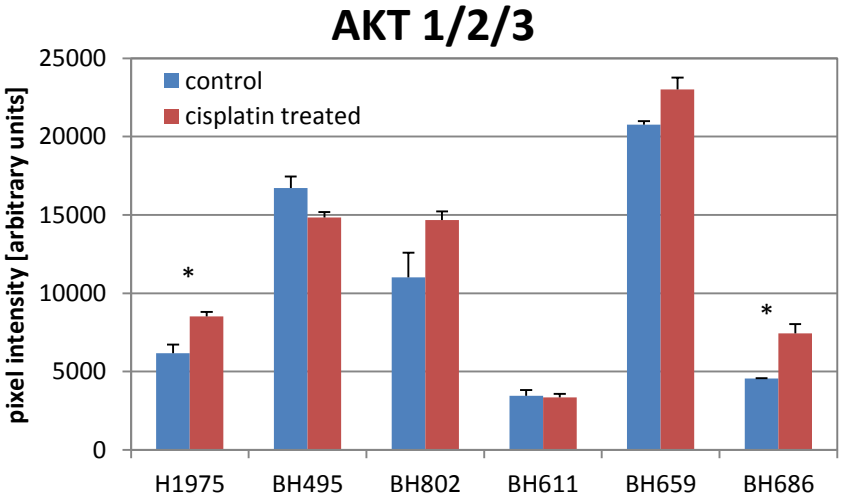

Figure 27 Comparison of the phosphorylation profile of AKT1/2/3 (T308). Data are shown as mean values ± SD. Statistical significance is indicated by *.

The stress kinase c-Jun was hyperphosphorylated in H1975, BH611 and BH686 when treated with cisplatin (Figure 28). BH495 and BH659 showed no significant alteration in phosphorylation. BH495, BH802 and BH659 exhibited an overall high basal phosphorylation in both groups.

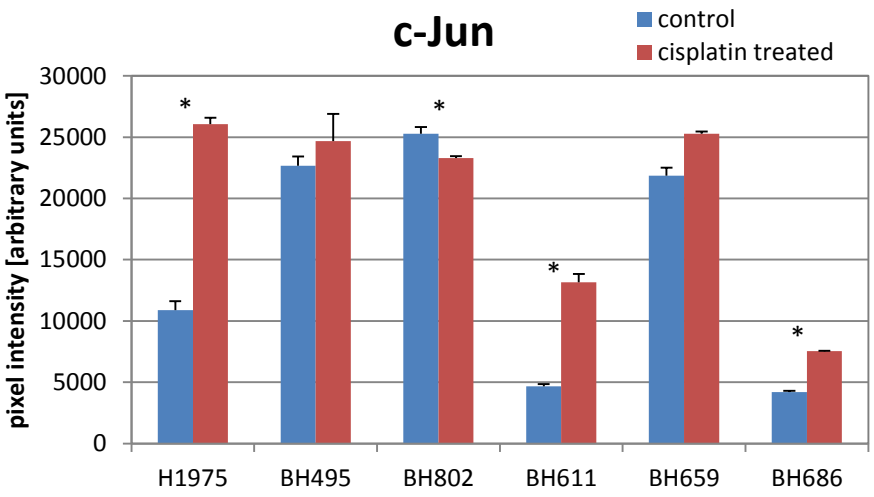

Figure 28 Comparison of the phosphorylation profile of c-Jun (S63). Data are shown as mean values ± SD. Statistical significance is indicated by *.

The phosphorylation of STAT3 at residue Y705 showed a significant difference in the cisplatin treated groups of H1975, BH495, BH802, BH659 and BH686 compared to the control groups (Figure 29). No difference of phosphorylation in BH611 was detected. BH659 showed the highest phosphorylation of STAT3 out of all cell lines. Again, compared to all other cell lines, BH611 and BH686 showed significantly lower phosphorylation of STAT3 in both groups.

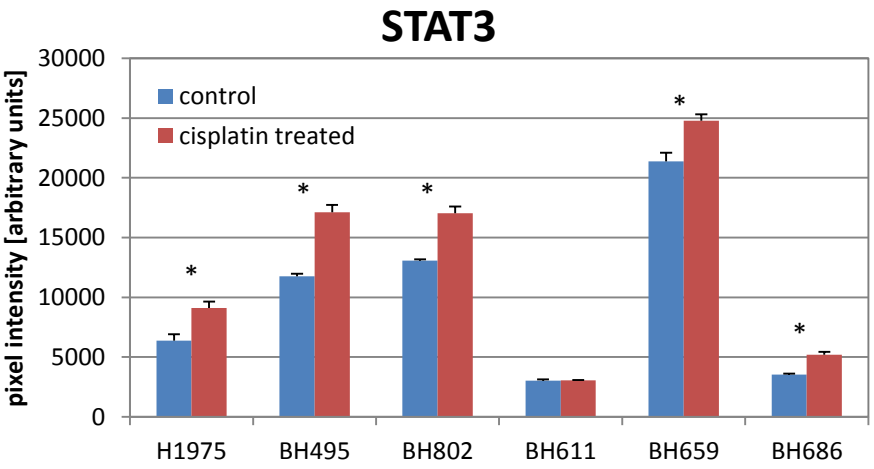

Figure 29 Comparison of the phosphorylation profile of STAT3 (Y705). Data are shown as mean values ± SD. Statistical significance is indicated by *.

The last protein shown in more detail is HSP60 (Figure 30). There was no definite phosphorylation site given for this protein as the total amount of protein was determined. All of the cell lines showed a significant difference in the level of protein expression for this heat shock protein upon exposure to cisplatin. BH611 was the only cell line which showed a reduction of the expression of HSP60 in cisplatin-treated cells. In BH495 the lowest level of HSP60 protein expression was found.

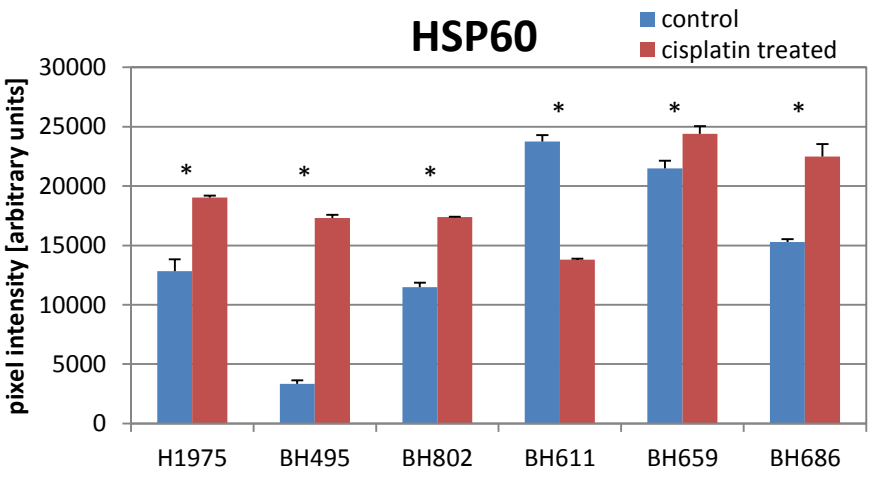

Figure 30 Comparison of the phosphorylation profile of HSP60. Data are shown as mean values ± SD. Statistical significance is indicated by *.

In order to set the differences in the level of phosphorylation and protein expression of the cell lines in context, the cisplatin IC_{50} values of the cell lines were plotted against the differences of the phosphorylation in the cisplatin-treated versus control group (Figure 31). For this figure, more significant proteins such as β-catenin, STAT2 and WNK1 were added.

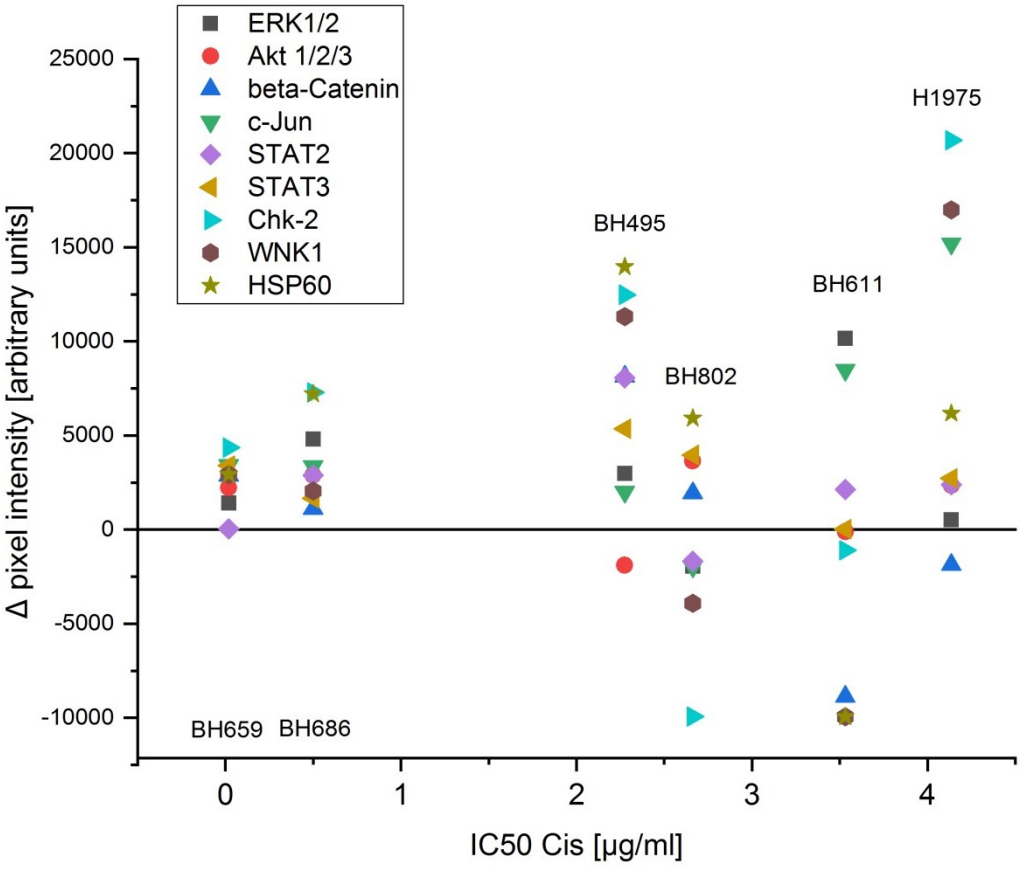

Figure 31 comparison of the IC_{50} and the difference of the level of phosphorylation for the cisplatin treated and the control from the Array of the different cell lines. The IC_{50} values for BH659 and BH686 are not according to scale, as they are very sensitive to cisplatin.

However, the response of the protein phosphorylation pattern was heterogeneous for the cell lines. There is no consistent change in cisplatin-triggered phosphorylation in these lung cancer cell lines. BH659 and BH686 showed a more homogeneous and lower change in phosphorylation for these proteins. The IC_{50} for these cell lines is not according to scale as these cell lines are so sensitive to cisplatin that an artificial value was presented for better visualization. The actual IC_{50} of BH659 and BH686 can be found in Figure 13. The change in the level of phosphorylation in the other cell lines is more widely scattered compared to BH659 and BH686. Chk-2 is hyperphosphorylated in H1975 and BH495 compared to BH802 and BH611. Although BH659 and BH686 are samples from the same patient, they show different changes in phosphorylation.

3.5 SCLC markers in transformed NSCLC cell lines

In order to determine the SCLC characteristics of potentially switched NSCLC cell lines, a qPCR with different markers that are known to be SCLC associated was performed. IVIC A, BH659 and BH686 were suspected to be SCLC transformed NSCLC cell lines. Therefore, these three cell lines were compared with S457, a SCLC cell line derived from pleura effusion. In Figure 32 a bar graph with the cycle threshold (Ct) mean of the different cell lines is shown. BH659 and BH686 yielded results comparable to S457. Only NCAM1 diverged from this pattern as this marker is not as highly expressed in BH659 as it is in S457 as more cycles are needed to see an expression. However, the expression of this marker is in cell line BH686 higher compared to BH659. IVIC A which has a partial NSCLC phenotype yielded a weaker expression for all markers compared to the other cell lines tested. Especially, CHGA and SYP are expressed at higher levels in the other cell lines compared to IVIC A. S457 and IVIC A showed a similar expression of EpCAM. Therefore, IVIC A, BH659 and BH686 reveal expression of typical SCLC markers thus indicating transformation.

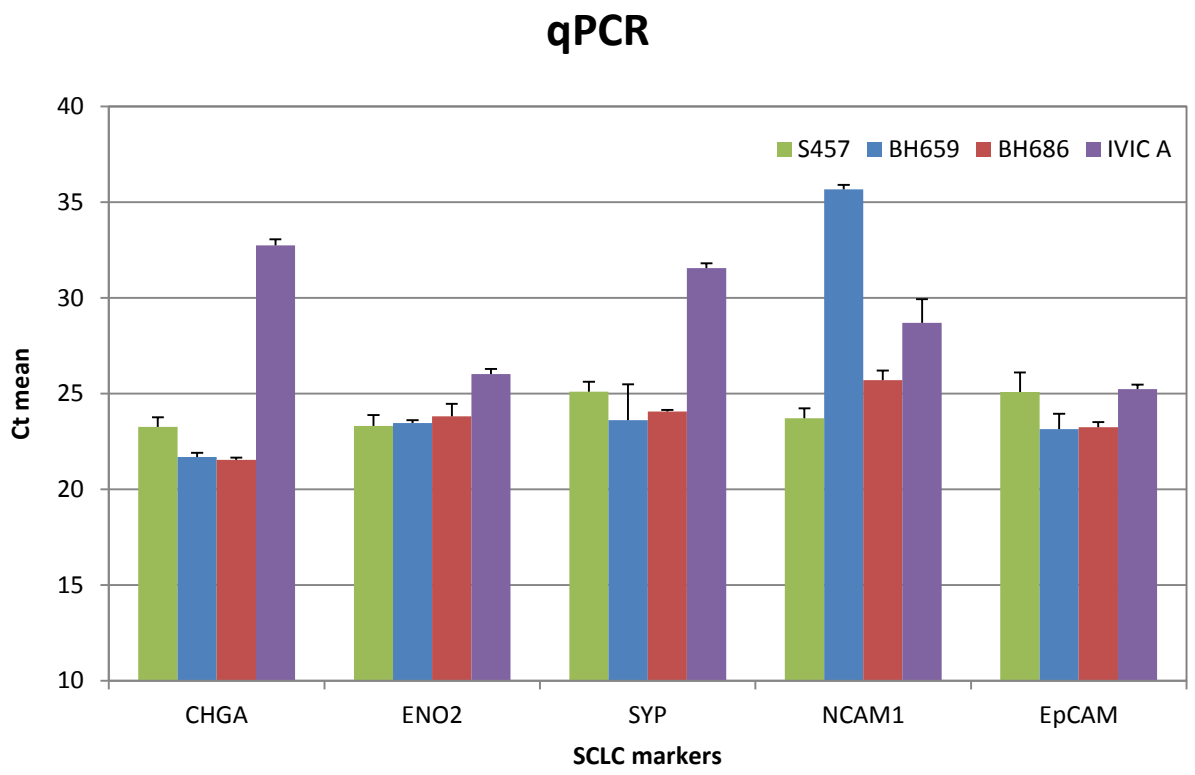

Figure 32 bar graph showing the ct mean of the different cell lines. Data are shown as mean values ± SD. Statistical significance is indicated by *.

4 Discussion

The traditional therapy for NSCLC consisted of cytotoxic chemotherapy applying platinum-based drug combinations including either docetaxel, pemetrexed or vincristine. However, response rates and PFS are poor resulting in 5-year survival rates of approximately 20%. The clinical results are even inferior for SCLC in comparison to NSCLC. Characterization of the genetic aberration of tumor cells yielded data on the mechanisms which cause the malign growth, either in form of oncogenes or downregulation of tumor suppressor genes and, in particular, the detection of a range of driver kinases found overexpressed in NSCLC. The most important of these enzymes are tyrosine kinases which can be inhibited in patients using specific inhibitors. Preferentially, TKIs target mutated kinases and normal tissues are largely spared. Due to this, the side effects of such targeted therapies are significantly smaller compared to conventional chemotherapy. The most frequent driver kinases in NSCLC comprise EGFR, ALK and ROS1 for which a range of first-line and second-line inhibitors are available (Rotow & Bivona, 2017). Patients invariably develop drug resistance to individual TKIs after 1-3 years and have to be treated accordingly with compounds active against the further mutated kinases. However, approximately 70% of patients do not develop a typical kinase mutation and express predictive markers for immunotherapy and, thus have to be treated by cytotoxic chemotherapy because markers for immunotherapy are missing. Furthermore, patients showing progression after using all available targeted agents have to be referred to cytotoxic therapy as a last resort of treatment.

Cytotoxic chemotherapy of NSCLC is largely ineffective, regardless of application in a primary setting or as rescue therapy. A lot of studies have been performed with permanent lung cancer cell lines which have been cultivated for prolonged time periods *in vitro* and, therefore may have lost typical characteristics present *in vivo*. To overcome this difficulty, lung cancer cells may be obtained from patients and kept as primary specimen for immediate testing. Metastatic lung cancer cells are prevalently present in pleural fluid which is drained to relieve breathing in patients. For the present, work a panel of these primary lung cancer cell lines was compared to several permanent NSCLC cell lines in respect to cisplatin sensitivity and effects of drug resistance modulators. The clinical marker screening has included kinase mutations and expression of PD-L1/tumor mutational burden, as an indicator of the sensitivity of positive patients to immunotherapy using one of several checkpoint inhibitor monoclonal antibodies (Goodman et al., 2017). Within the present study none of the pleural-derived cell lines has been tested positive for PD-L1 and, therefore, this immunotherapy approach could not be studied.

4.1 Cisplatin sensitivity

Cells were exposed to cisplatin and IC_{50} values calculated from dose-response curves. The mean chemosensitivities of the pleural cell lines and permanent cell lines to cisplatin was not significantly different and with IC_{50} values ranging from 3.64 to 2.9 µg/ml these values are near the plasma peak concentration (PPC) reported for this drug (approximately 3 µg/ml) and are expected to indicate chemoresistance of the cell lines tested (range: 0.82 – 9.45 µg/ml). Results for BH659 and BH686 were excluded from these calculations as both lines constitute highly sensitive NSCLC to SCLC transformed lung cancer lines. This observation correlates with the poor clinical results of chemotherapy in NSCLC.

4.1.1 Cisplatin & Chk1/2 inhibitor combination

Since the high IC_{50} values in most tested cell lines for cisplatin seem to indicate clinical refractoriness, several drugs which may increase the sensitivity to this chemotherapeutic were tested. One of the most adverse factors for the cisplatin cytotoxicity is the activation of DNA repair which may be inhibited by Chk1/2 inhibitors such as AZD-7762. As most of the malignant tumors lack the DNA damage checkpoint pathway in G1, they rely on S and G2 checkpoints in order to repair the DNA. However, by inhibiting the Chk1 signaling the repair is negatively affected resulting in increased tumor cell death. Furthermore, normal tissue has an efficient G1 checkpoint pathway which allows a normal repair of DNA and cell survival. Multiple xenograft models have indicated a dose dependent potentiation of antitumor activity if AZD-7762 is administered with DNA damaging agents (Zabludoff et al., 2008). Accordingly, the combination of AZD-7762 proved to be synergistic in 10 of 16 pleural NSCLC lines and the permanent H1299 line. However, 2 lines showed an additive effect and 4 lines exhibited marked antagonism of the AZD-7762/cisplatin combination.

4.1.2 Cisplatin & HSP90 inhibitor combination

Increased resistance to cisplatin may be associated with elevated expression of HSPs, including HSP90 which stabilizes the folding of mutated or damaged proteins (Krawczyk et al., 2018). STA9090, a potent inhibitor of HSP90, was tested in combination with cisplatin against the lung cancer cell lines (Proia & Bates, 2014). The present tests revealed that the STA9090/cisplatin combination showed low synergistic activity which was only present in 2 cell lines namely BH773 and BH833. Accordingly, STA9090 failed in clinical studies in cancer patients (Pillai et al., 2017).

4.1.3 Cisplatin & Nrf2 inhibitor combination

NSCLC often exhibits loss of function mutations in KEAP1 or gain of function mutations in NRF2 which have been associated with therapeutic induced resistance. ML385 blocks NRF2 resulting in inhibition of downstream target gene expression. Previous *in vitro* studies in NSCLC with a gain of function in NRF2 showed a significant antitumor activity when ML385 was administered in combination with carboplatin (Singh et al., 2016). However, with exception of the permanent H1299 NSCLC line, no synergistic effect could be detected for the ML385/cisplatin combination.

4.1.4 Cisplatin & niclosamide combination

Niclosamide has no explicit mode of action as this agent showed antiobesity, antidiabetic, antiviral and antisclerotic properties (Zuo et al., 2018). By inhibition of Wnt/β-catenin signaling, niclosamide initiate cell cycle arrest, inhibition of growth and apoptosis. Additionally, niclosamide decrease the formation of primary and secondary tumorspheres in SCLC (Wang et al., 2018). According to Liu et al., 2016, a combination of niclosamide and cisplatin could repress the growth of xenografts bred from MDA-MB-231. They also propose that niclosamide or in combination with cisplatin may be a potent therapeutic option for triple negative breast cancer.

Among the pleural NSCLC lines, niclosamide acted synergistically or additively with cisplatin in 7 out of 15 cell lines and was highly active in all four permanent cell lines. Niclosamide seems to influence signal transduction and cell survival pathways. Typically, the permanent cell lines which have been in culture for extended time periods were highly sensitive but the freshly isolated primary pleural NSCLC lines suggest that this anthelminthic may have very limited effects in patients.

4.1.5 Cisplatin & pristimerin combination

Pristimerin shows anticancer activity by inhibiting NFkB and AKT signaling pathways. Zhang et al., showed a retarded cell proliferation, induction of cell cycle arrest and apoptosis in two permanent NSCLC cell lines. In combination with cisplatin, pristimerin showed a synergistic effect resulting in increased cell death in cells and a suppression of growth *in vivo* xenografts (Zhang et al., 2019).

However, pristimerin only showed an additive effect in 4 out of 8 cell lines (2 pleural and 2 permanent cell lines). As this drug has no explicit mode of action, it can be assumed that the pleural cell lines reacts differently compared to the longer cultivated permanent cell lines. Therefore, this drug may have the same limited effects in patients.

4.2 3D cultures

Results of cytotoxicity tests in 2D cultures show a poor correlation with *in vivo* clinical results because this cellular arrangement does not reflect the actual tumor structure in patients (Hamilton & Rath, 2018). 3D cultures are better representations of *in vivo* conditions and have been initiated by prevention of the attachment of cancer cells to substrates by a range of methods. One of the simplest techniques is the cultivation of cells on an agarose layer which enforces a growth of the cancer cells in suspension and cell-cell adherence. However, 3D aggregates differ widely and may represent loose aggregates or large spheroids with hypoxic cores. In the present study some of the permanent and pleural NSCLC lines were kept in 3D cultures and exposed to cisplatin in MTT assays. Comparison of the IC_{50} values of 2D to 3D cultures revealed divergent results with 2 cell lines exhibiting higher resistance and a transformed line showing increased sensitivity. The modulation of cisplatin sensitivity by AZD-7762 resulted in synergy in 2 and antagonism in 2 other cases. The STA9090/cisplatin combinations revealed mostly synergism in 3D cultures, in contrast to the results obtained in 2D cultures. Similarly, niclosamide/cisplatin combinations showed mixed effects in 3D cultures with either decreased or increased chemosensitivity.

4.3 Human Phosphokinase Array

Exposure of cells to cisplatin activates intracellular signal transduction pathways to cope with the drug-induced stress. The phosphorylation status of key proteins in stress response was assayed in phosphoprotein Western blot arrays. Chk-2 is significantly hyperphosphorylated in response to cisplatin in most cell lines, except in lines which exhibit increased basal phosphorylation in controls. Activation of Chk-2 functions in activation of the DDR and cell protection. Similarly, the MAPK pathway is activated except in hyperphosphorylated controls as shown by ERK1/2 status. AKT1/2/3 becomes activated in cell lines with low primary phosphorylation in good correspondence with the stress kinase c-Jun. STAT3 is activated in most cell lines in response to cisplatin and HSP60 protein expression is increased. In summary, except for the NSCLC to SCLC transformed lines, the response in phosphoproteins is highly heterogeneous. As mentioned above, BH659 and BH686 revealed a high sensitivity to cisplatin. However, the phosphorylation response of the phosphoproteins is more confined in these two lines compared to the others. Although both lines are derived from the same patient taken 18 days apart from each other, the phosphorylation profile is slightly different. Transformed NSCLC to SCLC cell lines have different biological characteristics compared to the native NSCLC cancer cells.

4.4 SCLC markers in transformed NSCLC cell lines

Unfortunately, the histopathological diagnosis of SCLC can be difficult as this type of lung cancer has no distinctive morphology. However, the neuroendocrine markers CHGA, ENO2 and SYP are markers associated with SCLC cells (Obermayr et al., 2019). In order to characterize the possibly transformed NSCLC lines further they were analyzed by qPCR. The qPCR revealed an expression of the typical SCLC markers in both of these cell lines. We further tested the cell lines for NCAM1 and EpCAM. The similarity of S457 to BH659 and BH686 indicates a transformation from NSCLC to SCLC. IVIC A also revealed similar expression of the SCLC markers but it can be assumed that this cell line has not transformed completely to SCLC.

Immunotherapy using antibodies to checkpoint inhibitor proteins proved to be superior to chemotherapy in patients exhibiting significant expression of PD-1/PD-L1/CTLL4 or high tumor mutational burden which constitute an approximately 10% subpopulation of all NSCLC patients (Naidoo et al., 2015). The combination of immunotherapy with chemotherapy has been largely ruled out in the past due to presumed antagonistic effects on the immune effector cells. However, recent trials have demonstrated that immunochemotherapy is feasible and superior to chemotherapy alone but the expression of PD-1/PD-L1 has been shown to have no predictive power for immunochemotherapy. For example, according to Wang, Kulkarni & Salgia, the longer overall survival and PFS of platinum-doublet chemotherapy coupled with anti-PD-L1 drugs such as pembrolizumab was independent of PD-L1 expression in the tumor. Additionally, EGFR mutant NSCLC patients do not benefit from a treatment with PD-1 or PD-L1 inhibitors (Wang, Kulkarni & Salgia, 2019). Such results have been explained as stimulation of the activities of the immune system by chemotherapeutic-triggered lysis of tumor cells and release of neoantigens and by removal of suppressive immune cell populations (Tregs or myeloid-derived suppressor cells) by chemotherapy. The results of the present work may help to define and select suitable patients for immunochemotherapy: high chemoresistance of NSCLC cells seems to indicate resistance to cell lysis, release of neoantigens and stimulation of the immune system. Since it may not be possible to obtain pleural effusions of some NSCLC patients and to test chemosensitivity, indirect indicators such as the hyperphosphorylated status of proteins involved in resistance may be detected in tumor biopsies. Thus, Chk-2 or stress kinase c-Jun might be suitable markers as the results show a hyperphosphorylation in all highly resistant cell lines tested. In conclusion, 2D and 3D cultures of pleural primary NSCLC cells exhibit high chemoresistance to cisplatin which could not be reversed with the range of modulators tested in the present work.

5 References

American Cancer Society (2019) 5-year relative survival rates for small cell lung cancer. Retrieved August 1, 2019, from https://www.cancer.org/cancer/small-cell-lung-cancer/detection-diagnosis-staging/survival-rates.html

Ancevski Hunter K, Socinski MA & Villaruz LC (2018) PD-L1 Testing in Guiding Patient Selection for PD-1/PD-L1 Inhibitor Therapy in Lung Cancer. *Mol Diagn Ther* **22**(1):1-10.

Austrian society of pneumology (2019) Lungenkrebs in Österreich – Bei Behandlung und Forschung führend, Neuerkrankungen nehmen aber vor allem bei Frauen dramatisch zu! Retrieved August 12, 2019, from https://www.ogp.at/lungenkrebs-in-oesterreich-bei-behandlung-und-forschung-fuehrend-neuerkrankungen-nehmen-aber-vor-allem-bei-frauen-dramatisch-zu/

Chan BA & Hughes BGM (2015) Targeted therapy for non-small cell lung cancer: current standards and the promise of the future. *Transl Lung Cancer Res* **4**(1):36-54

Chen N, Fang W, Zhan J, Hong S, Tang Y, Kang S, Zhang Y, He X, Zhou T, Qin T, Huang Y, Yi X & Zhang L (2015) Upregulation of PD-L1 by EGFR activation mediates the immune escape in EGFR-driven NSCLC: Implication for optional immune targeted therapy for NSCLC patients with EGFR mutation. *J Thorac Oncol* **10**(6):910-23

Chou TC (2010) Drug combination studies and their synergy quantification using the chou-talalay method. Cancer Research. *Cancer Res* **70**(2):440-6

Dela Cruz CS, Tanoue LT & Matthay RA (2011) Lung Cancer: Epidemiology, Etiology, and Prevention. *Clin Chest Med* **32**(4):605-44

Dorantes-Heredia R, Ruiz-Morales JM & Cano-García F (2016) Histopathological transformation to small-cell lung carcinoma in non-small cell lung carcinoma tumors. *Transl Lung Cancer Res* **5**(4):401-12

Dutt A, Ramos AH, Hammerman PS, Mermel C, Cho J, Sharifnia T, Chande A, Tanaka KE, Stransky N, Greulich H, Gray NS & Meyerson M (2011). Inhibitor-sensitive fgfr1 amplification in human non-small cell lung cancer. *PLoS One* **6**(6):e20351

Feng J, Yang H, Zhang Y, Wei H, Zhu Z, Zhu B, Yang M, Cao W, Wang L & Wu Z. (2017). Tumor cell-derived lactate induces TAZ-dependent upregulation of PD-L1 through GPR81 in human lung cancer cells. *Oncogene* **36**(42):5829-5839

Galluzzi L, Vitale I, Michels J, Brenner C, Szabadkai G, Harel-Bellan A, Castedo M & Kroemer G (2014) Systems biology of cisplatin resistance: Past, present and future. *Cell Death Dis* **5**:e1257

Goodman AM, Kato S, Bazhenova L, Patel SP, Frampton GM, Miller V, Stephens PJ, Daniels GA & Kurzrock R (2017) Tumor Mutational Burden as an Independent Predictor of Response to Immunotherapy in Diverse Cancers. *Mol Cancer Ther* **16**(11):2598-2608

Guarino M (2010) Src signaling in cancer invasion. *J Cell Physiol* **223**(1):14-26

Hamilton G & Rath B (2014) A short update on cancer chemoresistance. *Wien Med Wochenschr* **164**(21-22):456-60

Hamilton G & Rath B (2017). Repurposing of Anthelminthics as Anticancer Drugs. *Oncomed* **3**:1-8

Hamilton G & Rath B (2018) Applicability of tumor spheroids for in vitro chemosensitivity assays. *Expert Opin Drug Metab Toxicol* **15**(1):15-23

Hamilton G & Rath B (2019) Role of circulating tumor cell spheroids in drug resistance. *Cancer Drug Resist* **2**:762-772

Hamilton G, Rath B, Plangger A & Hochmair M (2019) Implementation of functional precision medicine for anaplastic lymphoma kinase-rearranged non-small lung cancer. *Precis Cancer Med* **2**:19

Hanahan D & Weinberg RA (2000) The hallmarks of cancer. *Cell* **100**(1):57-70.

Hanahan D & Weinberg RA (2011) Hallmarks of cancer: the next generation. *Cell* **144**(5):646-74

Herbst RS, Baas P, Kim DW, Felip E, Pérez-Gracia JL, Han JY, Molina J, Kim JH, Arvis CD, Ahn MJ, Majem M, Fidler MJ, de Castro G Jr, Garrido M, Lubiniecki GM, Shentu Y, Im E, Dolled-Filhart M & Garon EB (2016) Pembrolizumab versus docetaxel for previously treated, PD-L1-positive, advanced non-small-cell lung cancer (KEYNOTE-010): A randomised controlled trial. *Lancet* **387**(10027):1540-1550

Herbst RS, Heymach JV & Lippman SM (2008) Molecular Origins: Lung cancer. *N Engl J Med* **359**:1367-1380

Holohan C, Van Schaeybroeck S, Longley DB & Johnston PG (2013) Cancer drug resistance: An evolving paradigm. *Nat Rev Cancer* **13**(10):714-26

Housman G, Byler S, Heerboth S, Lapinska K, Longacre M, Snyder N & Sarkar S (2014) Drug resistance in cancer: An overview. *Cancers (Basel)* **6**(3):1769-92

Jain RK & Chen H (2017) Spotlight on brigatinib and its potential in the treatment of patients with metastatic ALK-positive non-small cell lung cancer who are resistant or intolerant to crizotinib. *Lung Cancer (Auckl)* **8**:169-177

Jhaveri K & Modi S (2015) Ganetespib: Research and clinical development. *Onco Targets Ther* **8**:1849-58

Klameth L, Rath B, Hochmaier M, Moser D, Redl M, Mungenast F, Gelles K, Ulsperger E, Zeillinger R & Hamilton G (2017) Small cell lung cancer: model of circulating tumor cell tumorospheres in chemoresistance. *Sci Rep* **7**(1):5337.

Knight SB, Crosbie PA, Balata H, Chudziak J, Hussell T & Dive C (2017) Progress and prospects of early detection in lung cancer. *Open Biol* **7**(9). pii: 170070

Kohno T, Nakaoku T, Tsuta K, Tsuchihara K, Matsumoto S, Yoh K & Goto K (2015) Beyond ALK-RET, ROS1 and other oncogene fusions in lung cancer. *Transl Lung Cancer Res* **4**(2):156-64

Krawczyk Z, Gogler-Pigłowska A, Sojka DR & Scieglinska D (2018) The Role of Heat Shock Proteins in Cisplatin Resistance. *Anticancer Agents Med Chem* **18**(15):2093-2109

Landau HJ, McNeely SC, Nair JS, Comenzo RL, Asai T, Friedman H, Jhanwar SC, Nimer SD & Schwartz GK (2012) The Checkpoint Kinase Inhibitor AZD7762 Potentiates Chemotherapy-Induced Apoptosis of p53-Mutated Multiple Myeloma Cells. *Mol Cancer Ther* **11**(8):1781-8.

Lee DH (2017) Treatments for EGFR-mutant non-small cell lung cancer (NSCLC): The road to a success, paved with failures. *Pharmacol Ther* **174**:1-21

Li Y, Li F, Jiang F, Lv X, Zhang R, Lu A & Zhang G (2016). A mini-review for cancer immunotherapy: Molecular understanding of PD-1/ PD-L1 pathway & translational blockade of immune checkpoints. *Int J Mol Sci* **17**(7). pii: E1151.

Li Z, Hu C, Zhen Y, Pang B, Yi H & Chen X (2019) Pristimerin inhibits glioma progression by targeting AGO2 and PTPN1 expression via miR-542-5p. *Biosci Rep* **39**(5). pii: BSR20182389

Liu J, Chen X, Ward T, Pegram M & Shen K (2016) Combined niclosamide with cisplatin inhibits epithelial-mesenchymal transition and tumor growth in cisplatin-resistant triple-negative breast cancer. *Tumour Bio* **37**(7):9825-35

Liu X, Wang P, Zhang C & Ma Z (2017) Epidermal growth factor receptor (EGFR): A rising star in the era of precision medicine of lung cancer. *Oncotarget* **8**(30):50209-50220

Liu Y, Ye X, Yu Y & Lu S (2019) Prognostic significance of anaplastic lymphoma kinase rearrangement in patients with completely resected lung adenocarcinoma. *J Thorac Dis* **11**(10):4258-4270

Mansoori B, Mohammadi A, Davudian S, Shirjang S & Baradaran B (2017) The different mechanisms of cancer drug resistance: A brief review. *Adv Pharm Bull* **7**(3):339-348

Naidoo J, Page DB, Li BT, Connell LC, Schindler K, Lacouture ME, Postow MA & Wolchok JD (2015) Toxicities of the anti-PD-1 and anti-PD-L1 immune checkpoint antibodies. *Ann Oncol* **26**(12):2375-91

Obermayr E, Agreiter C, Schuster E, Fabikan H, Weinlinger C, Baluchova K, Hamilton G, Hochmair M & Zeillinger R (2019) Molecular Characterization of Circulating Tumor Cells Enriched by A Microfluidic Platform in Patients with Small-Cell Lung Cancer. *Cells* **8**(8). pii: E880

Oser MG, Niederst MJ, Sequist LV & Engelman JA (2015). Transformation from non-small-cell lung cancer to small-cell lung cancer: Molecular drivers and cells of origin. *Lancet Oncol* **16**(4):e165-72.

Osmani L, Askin F, Gabrielson E & Li QK (2018) Current WHO guidelines and the critical role of immunohistochemical markers in the subclassification of non-small cell lung carcinoma (NSCLC): Moving from targeted therapy to immunotherapy. *Semin Cancer Biol* **52**(Pt 1):103-109

Proia DA & Bates RC (2014) Ganetespib and HSP90: Translating preclinical hypotheses into clinical promise. *Cancer Res* **74**(5):1294-300

Pillai R, Fennell D, Kovcin V, Ciuleanu T, Ramlau R, Kowalski R, Schenker M, Perin B, Yalcin I, Teofilovici F, Vukovic V & Ramalingam S (2017) PL03.09: Phase 3 Study of Ganetespib, a Heat Shock Protein 90 Inhibitor, with Docetaxel versus Docetaxel in Advanced Non-Small Cell Lung Cancer (GALAXY-2) *J Thorac Oncol* **12**(1):7-8

Radaram B, Pisaneschi F, Rao Y, Yang P, Piwnica-Worms D & Alauddin MM (2019) Novel derivatives of anaplastic lymphoma kinase inhibitors: Synthesis, radiolabeling, and preliminary biological studies of fluoroethyl analogues of crizotinib, alectinib, and ceritinib. *Eur J Med Chem* **182**:111571

Rajamuthiah R, Fuchs BB, Conery AL, Kim W, Jayamani E, Kwon B, Ausubel FM & Mylonakis E (2015) Repurposing salicylanilide anthelmintic drugs to combat drug resistant Staphylococcus aureus. *PLoS One* **10**(4):e0124595

Rocha C, Silva M, Quinet A, Cabral-Neto J & Menck C (2018) DNA repair pathways and cisplatin resistance: an intimate relationship. *Clinics (Sao Paulo)* **73**(Suppl 1): e478s.

Rooney M, Devarakonda S & Govindan R (2013) Genomics of Squamous Cell Lung Cancer. *Oncologist* **18**(6): 707–716.

Rotow J & Bivona TG (2017) Understanding and targeting resistance mechanisms in NSCLC. *Nat Rev Cancer* **17**(11):637-658

Shaw AT, Felip E, Bauer TM, Besse B, Navarro A, Postel-Vinay S, Gainor JF, Johnson M, Dietrich J, James LP, Clancy JS, Chen J, Martini JF, Abbattista & Solomon BJ (2017). Lorlatinib in non-small-cell lung cancer with ALK or ROS1 rearrangement: an international, multicentre, open-label, single-arm first-in-man phase 1 trial. *Lancet Oncol*. **18**(12): 1590–1599.

Sigma Aldrich Co. LLC (2019) ML385. Retrieved February 5, 2019, from https://www.sigmaaldrich.com/catalog/product/sigma/sml1833?lang=de&region=AT

Singh A, Venkannagari S, Oh KH, Zhang YQ, Rohde JM, Liu L, Nimmagadda S, Sudini K, Brimacombe KR, Gajghate S, Ma J, Wang A, Xu X, Shahane SA, Xia M, Woo J, Mensah GA, Wang Z, Ferrer M, Gabrielson E, Li Z, Rastinejad F, Shen M, Boxer MB & Biswal S (2016) Small Molecule Inhibitor of NRF2 Selectively Intervenes Therapeutic Resistance in KEAP1-Deficient NSCLC Tumors. *ACS Chem Biol* **11**(11):3214-3225.

Song MA, Benowitz NL, Berman M, Brasky TM, Cummings KM, Hatsukami DK, Marian C, O'Connor R, Rees VW, Woroszylo C & Shields PG (2017) Cigarette Filter Ventilation and its Relationship to Increasing Rates of Lung Adenocarcinoma. *J Natl Cancer Inst* **109**(12):djx075

Stathopoulou A, Gizi A, Perraki M, Apostolaki S, Malamos N, Mavroudis D, Georgoulias V & Lianidou ES (2003) Real-Time Quantification of CK-19 mRNA-Positive Cells in Peripheral Blood of Breast Cancer Patients Using the Lightcycler System. *Clin Cancer Res* **9**(14):5145-51

Statistics Austria (2007) Raucheranteil der Bevölkerung nach Bundesländern und Geschlecht in den Jahren 1979, 1986 und 1997. Retrieved July 22, 2019, from https://www.statistik.at/web_de/statistiken/menschen_und_gesellschaft/gesundheit/gesundheitsdeterminanten/rauchen/022253.html

Statistics Austria (2015) Aktueller Raucherstatus 2014. Retrieved July 22, 2019, from https://www.statistik.at/web_de/statistiken/menschen_und_gesellschaft/gesundheit/gesundheitsdeterminanten/rauchen/105592.html

Statistics Austria (2018a) Luftröhre, Bronchien und Lunge (C33-C34) - Krebsinzidenz (Neuerkrankungen pro Jahr). Retrieved December 7, 2018, from https://www.statistik.at/web_de/statistiken/menschen_und_gesellschaft/gesundheit/krebserkrankungen/luftroehre_bronchien_lunge/021766.html

Statistics Austria (2018b) Luftröhre, Bronchien und Lunge (C33-C34) - Krebsmortalität (Sterbefälle pro Jahr). Retrieved December 7, 2018, from https://www.statistik.at/web_de/statistiken/menschen_und_gesellschaft/gesundheit/krebserkrankungen/luftroehre_bronchien_lunge/021767.html

Statistics Austria (2019) Luftröhre, Bronchien, Lunge. Retrieved July 23, 2019, from https://www.statistik.at/web_de/statistiken/menschen_und_gesellschaft/gesundheit/krebserkrankungen/luftroehre_bronchien_lunge/index.html

Tsvetkova E & Goss GD (2012) Drug resistance and its significance for treatment decisions in non-small-cell lung cancer. *Curr Oncol* **19**(Suppl 1):S45–S51.

Vasan N, Baselga J & Hyman DM (2019) A view on drug resistance in cancer. *Nature* **575**:299–309

Wang C, Kulkarni P & Salgia R (2019) Combined Checkpoint Inhibition and Chemotherapy: New Era of 1 st -Line Treatment for Non-Small-Cell Lung Cancer. *Mol Ther Oncolytics* **13**:1–6

Wang LH, Xu M, Fu LQ, Chen XY & Yang F (2018) The Antihelminthic Niclosamide Inhibits Cancer Stemness, Extracellular Matrix Remodeling, and Metastasis through Dysregulation of the Nuclear β-catenin/c-Myc axis in OSCC. *Sci Rep* **8**(1):12776

Wang X, Zhang H & Chen X (2019) Drug resistance and combating drug resistance in cancer. *Cancer Drug Resist* **2**:141-160

Weiswald LB, Bellet D & Dangles-Marie V (2015) Spherical Cancer Models in Tumor Biology. *Neoplasia* **17**(1):1–15.

WHO (2018) Cancer. Retrieved June 12, 2019, from https://www.who.int/news-room/fact-sheets/detail/cancer

Wind S, Schnell D, Ebner T, Freiwald M & Stopfer P (2016) Clinical Pharmacokinetics and Pharmacodynamics of Afatinib. *Clin Pharmacokinet* **56**(3):235–250.

Wu J, Savooji J & Liu D (2016) Second- and third-generation ALK inhibitors for non-small cell lung cancer. *J Hematol Oncol* **9**:19.

Zabludoff SD, Deng C, Grondine MR, Sheehy AM, Ashwell S, Caleb BL, Green S, Haye HR, Horn CL, Janetka JW, Liu D, Mouchet E, Ready S, Rosenthal JL, Queva C, Schwartz GK, Taylor KJ, Tse AN, Walker GE & White AM. (2008). AZD7762, a novel checkpoint kinase inhibitor, drives checkpoint abrogation and potentiates DNA-targeted therapies. *Mol Cancer Ther* **7**(9):2955-66

Zhang Y, Wang J, Hui B, Sun W, Li B, Shi F, Che S, Chai L & Song L (2019) Pristimerin enhances the effect of cisplatin by inhibiting the miR-23a/Akt/GSK3β signaling pathway and suppressing autophagy in lung cancer cells. *Int J Mol Med* **43**(3):1382-1394

Zuo Y, Yang D, Yu Y, Xiang M, Li H, Yang J, Li J, Jiang D, Zhou H, Xu Z & Yu Z (2018) Niclosamide enhances the cytotoxic effect of cisplatin in cisplatin-resistant human Lung cancer cells via suppression of Lung resistance-related protein and c-myc. *Mol Med Rep* **17**(3):3497-3502

6 List of figures

7 Appendix

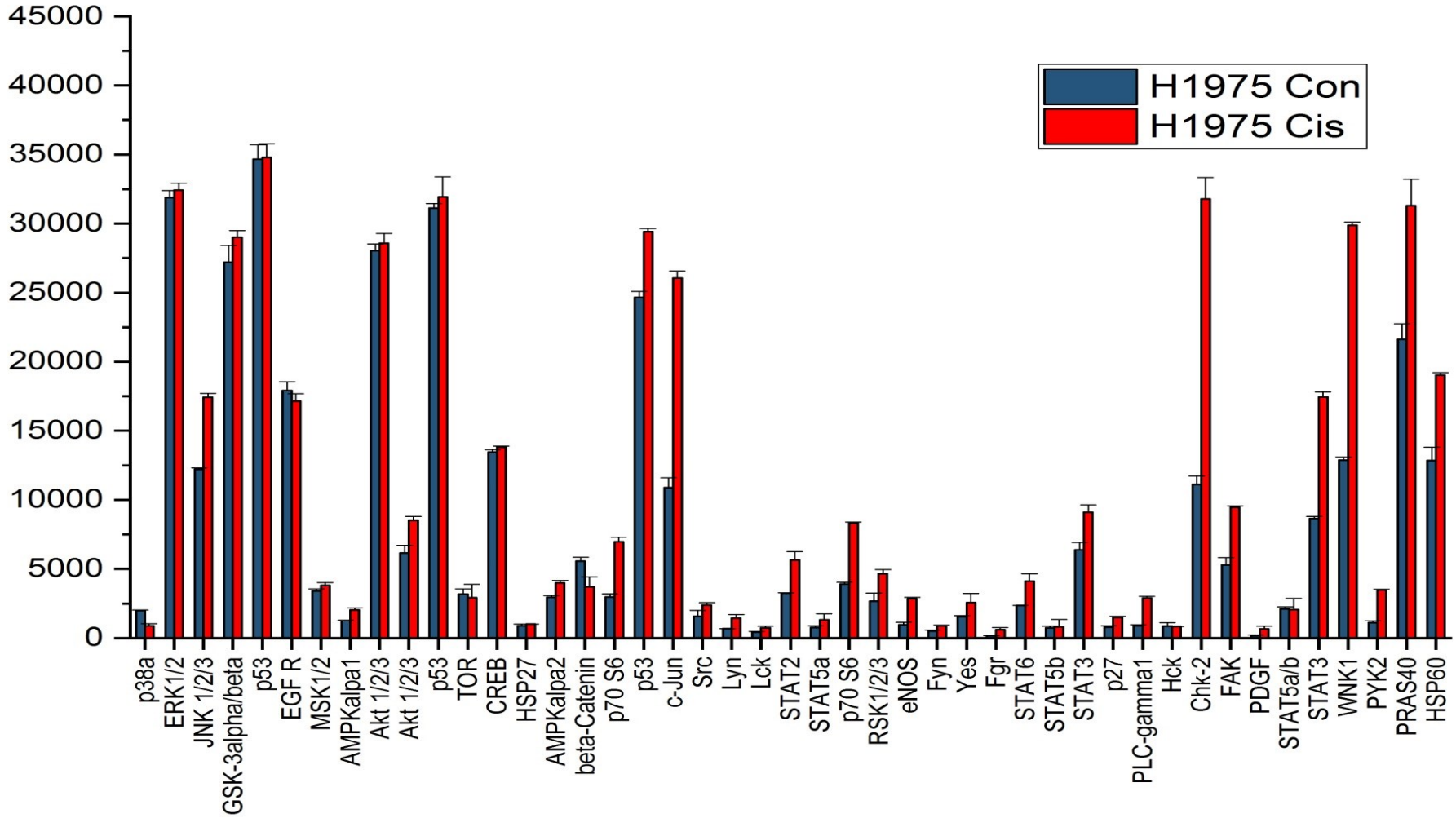

Figure 33 Human Phosphokinase Array ARY003B of cell line H1975.

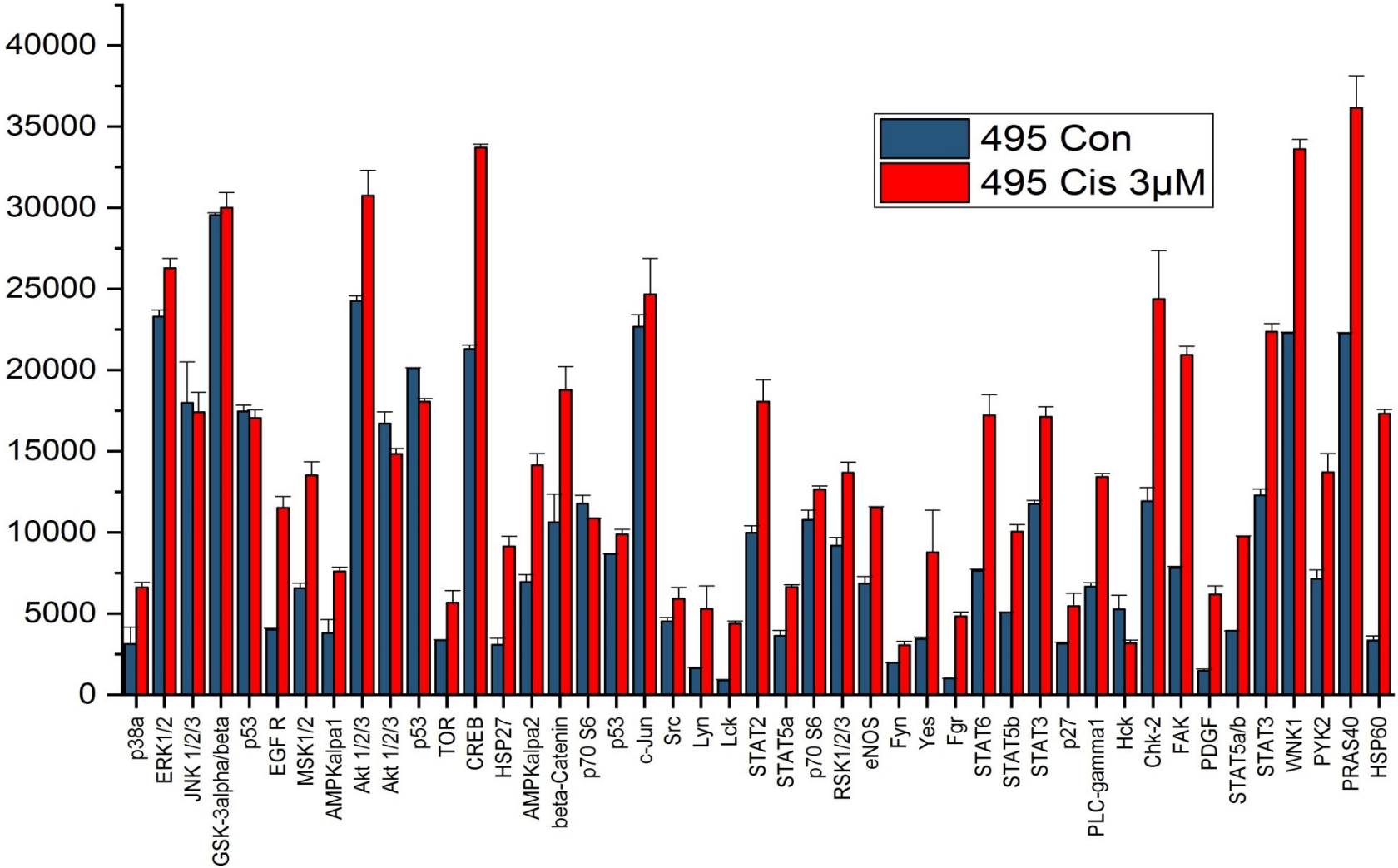

Figure 34 Human Phosphokinase Array ARY003B of cell line BH495.

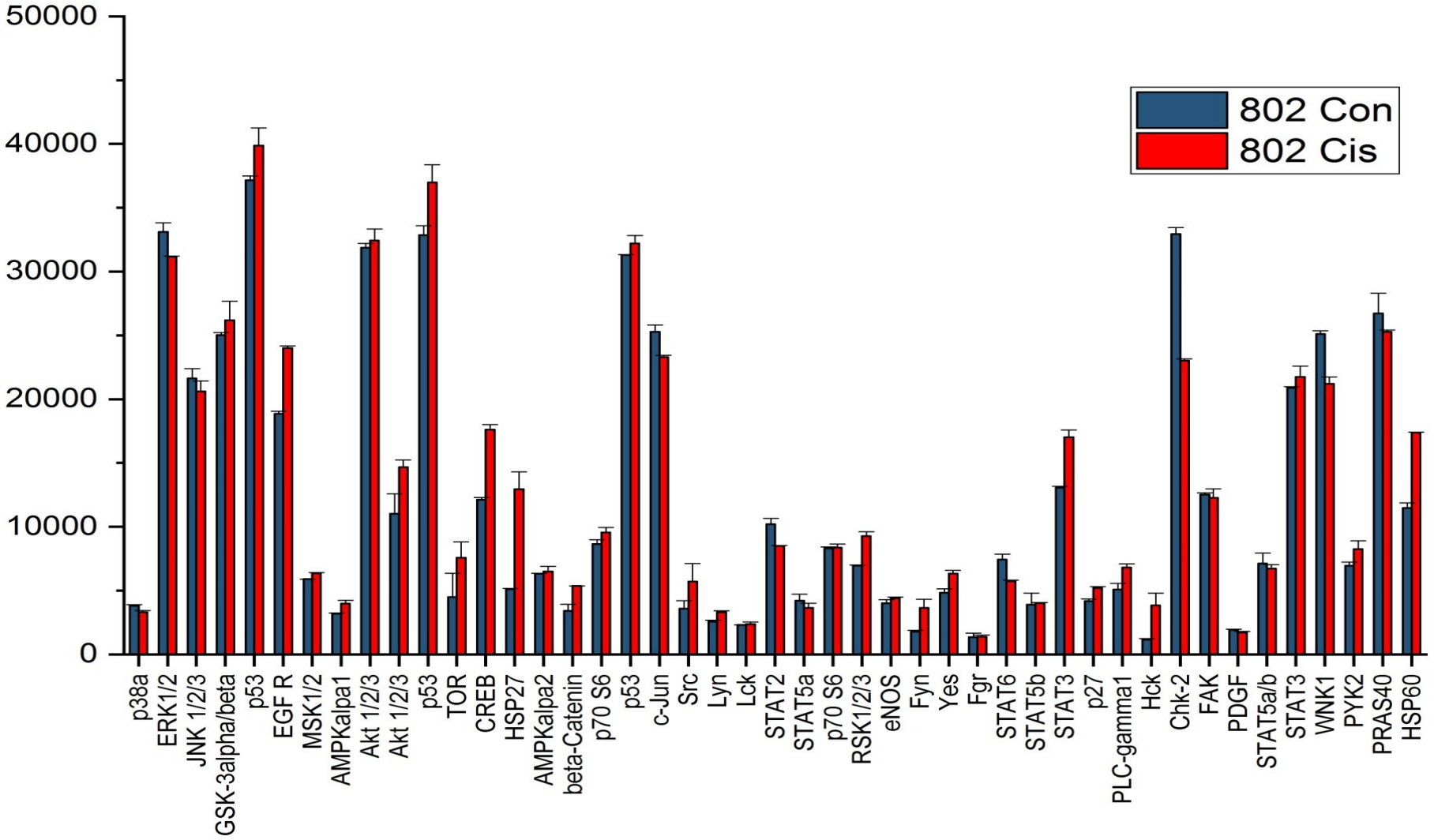

Figure 35 Human Phosphokinase Array ARY003B of cell line BH802.

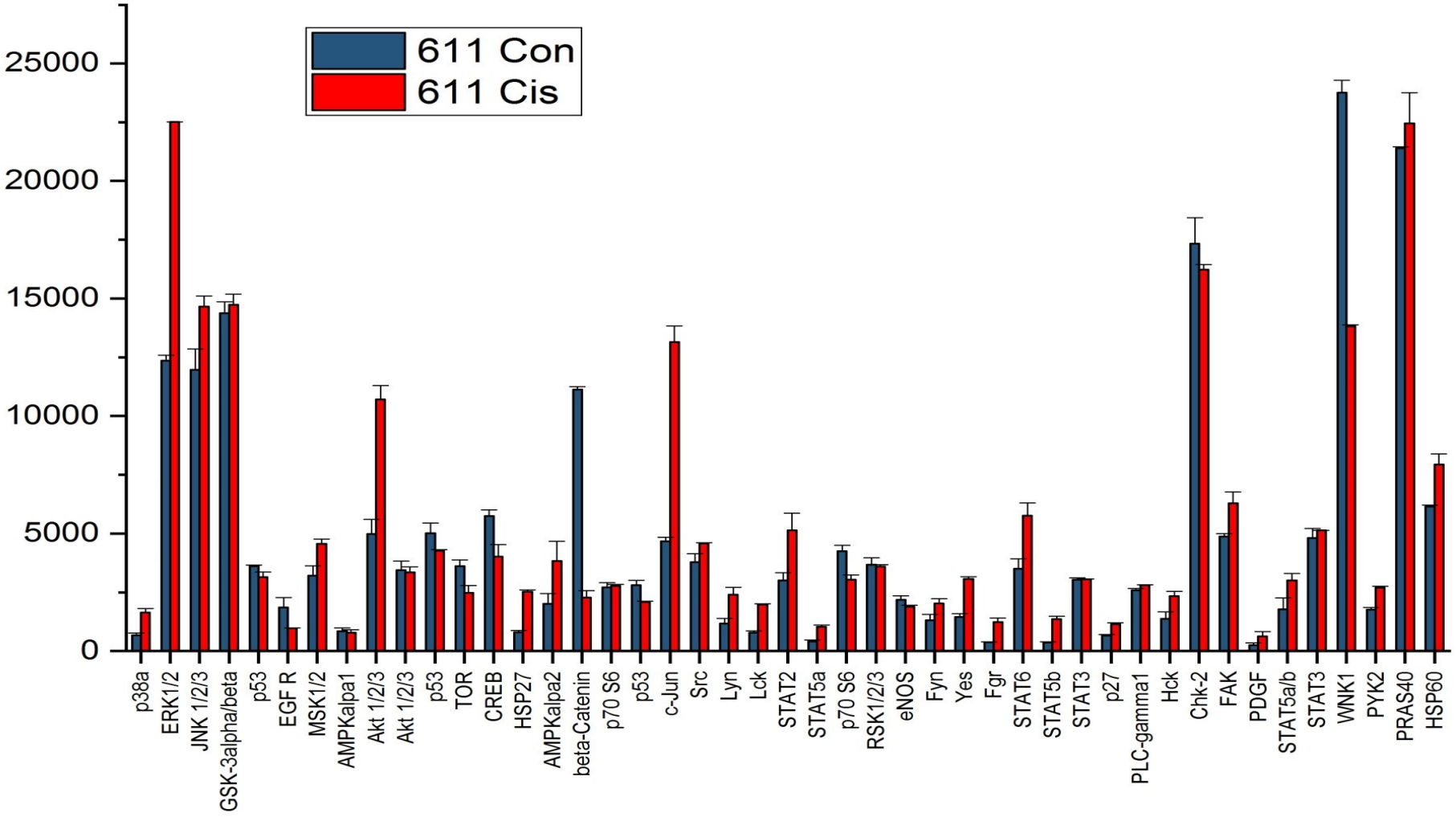

Figure 36 Human Phosphokinase Array ARY003B of cell line BH611.

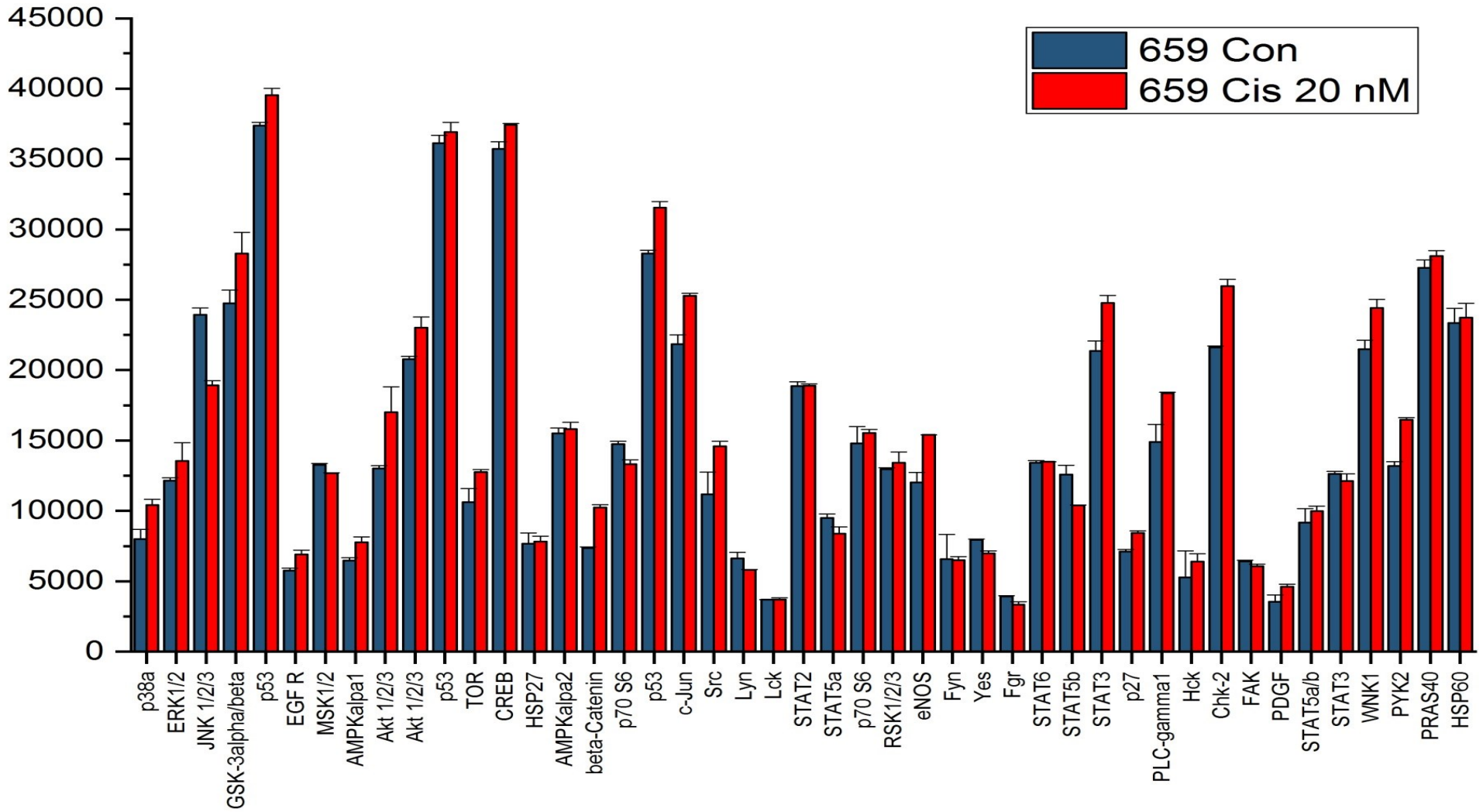

Figure 37 Human Phosphokinase Array ARY003B of cell line BH659.

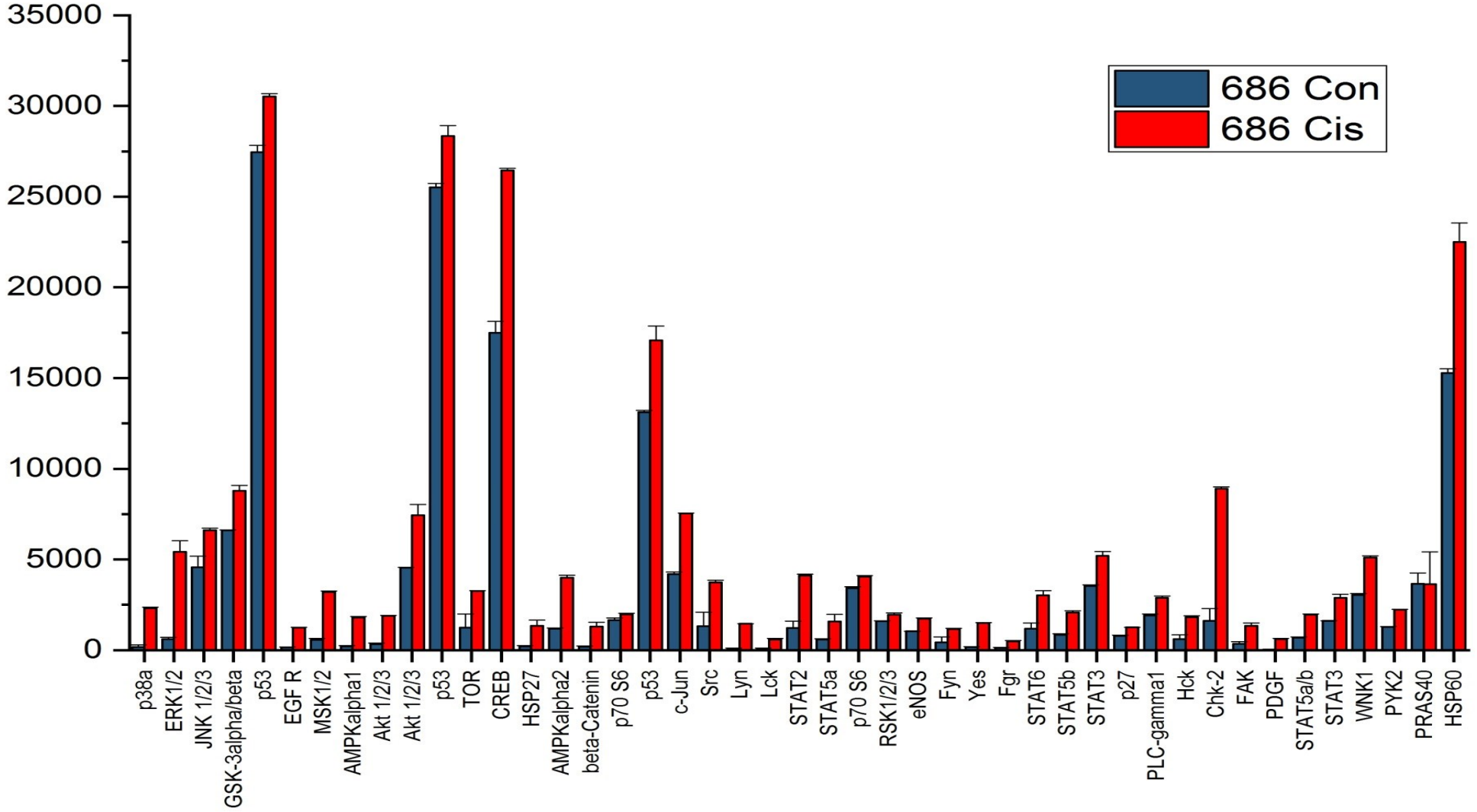

Figure 38 Human Phosphokinase Array ARY003B of cell line BH686.